NASA Special Publication 513

Selected Examples of NACA/NASA Supersonic Flight Research

Edwin J. Saltzman and Theodore G. Ayers

May 1995

National Aeronautics and
Space Administration

NASA Special Publication 513

Selected Examples of NACA/NASA Supersonic Flight Research

Edwin J. Saltzman
PRC Inc.
Edwards, CA 93523-0273

Theodore G. Ayers
NASA Dryden Flight Research Center
Edwards, CA 93523-0273

1995

National Aeronautics and
Space Administration

Dryden Flight Research Center
Edwards, California 93523-0273

CONTENTS

ABSTRACT 1

NOMENCLATURE 1

INTRODUCTION 5

DISCUSSION 6
Stage 1: Barriers to Supersonic Flight 6
The Adjustable "All-Movable" Stabilizer 9
The Identification of Inertial Coupling 10
The Area Rule: Reducing the Magnitude of the Wave-Drag Barrier 12
Reaction Controls: The Problem of Control at Low Dynamic Pressure 16
Summary of Stage 1: Barriers to Supersonic Flight 20
Stage 2: Correlation–Integration of Ground Facility Data and Flight Data 20
Supersonic Wind-Tunnel Model-to-Flight Drag Correlation 20
Wall Interference and Flexibility Effects 22
The "Cold-Wall" Experiment: A Direct Wind Tunnel-to-Flight Correlation 27
Correlation of Flight and Wind-Tunnel Flow Quality 29
Aero-Thermal Structures Research 34
Parameter Estimation: A Powerful Tool for Flight-to-Wind-Tunnel Model Data Correlation 38
Summary of Stage 2: Correlation–Integration of Ground Facility Data and Flight Data 41
Stage 3: Integration of Disciplines 41
Propulsion Control and Integration 41
Mach-Three-Cruise Flightpath Control 46
Digital Fly-By-Wire 48
Summary of Stage 3: Integration of Disciplines 51

CONCLUDING REMARKS 51

ACKNOWLEDGMENTS 52

REFERENCES 52

TABLE 58
Listing of stages of supersonic flight research and thirteen selected examples 58

DEDICATION

The authors dedicate this Special Publication to the memory of their valued friend and coworker, Milton O. Thompson. Milt was a pioneering research pilot for NASA, having flown the X-15 hypersonic research aircraft 14 times over a 22 month period. Milt was also the first lifting-body pilot and made many technical contributions to the development of low lift-to-drag ratio vehicles. The experience gained from these early lifting-body flights was later of significant value in the development of the Space Shuttle. Milt passed away suddenly on August 6, 1993 at which time he was serving as Chief Engineer of the NASA Dryden Flight Research Facility.

ABSTRACT

The present Dryden Flight Research Center,* a part of the National Aeronautics and Space Administration, has a flight research history that extends back to the mid-1940's. The parent organization was a part of the National Advisory Committee for Aeronautics and was formed in 1946 as the Muroc Flight Test Unit.

This document describes 13 selected examples of important supersonic flight research conducted from the Mojave Desert location of the Dryden Flight Research Facility over a 4 decade period beginning in 1946. The research described herein was either obtained at supersonic speeds or enabled subsequent aircraft to penetrate or traverse the supersonic region. In some instances there accrued from these research efforts benefits which are also applicable at lower or higher speed regions. A major consideration in the selection of the various research topics was the lasting impact they have had, or will have, on subsequent supersonic flight vehicle design, efficiency, safety, and performance or upon improved supersonic research techniques.

NOMENCLATURE

CBS	computer bypass system
DEEC	digital electronic engine control
DFWB	digital fly-by-wire
DFRF	Dryden Flight Research Facility, Edwards, CA
HIDEC	highly integrated digital electronic control
HiMAT	highly maneuverable aircraft technology
IFU	interface unit associated with DFBW control system
IPCS	integrated propulsion control system
NACA	National Advisory Committee for Aeronautics
NASA	National Aeronautics and Space Administration
SCW	supercritical wing
TACT	transonic aircraft technology
TRF	Thermostructures Research Facility, DFRF

The following acronyms identify wind tunnels in support of figure 23

AEDC	Arnold Engineering Development Center, Tullahoma, TN
HSST	High-Speed Supersonic Tunnel
NPL	National Physical Laboratory

*During the time that this document was being written, revised, and undergoing technical and editorial review the sponsoring organization was the NASA Dryden Flight Research Facility. On March 1, 1994, Dryden became, again, the NASA Dryden Flight Research Center. Most references to the organization in the text will remain as "Facility" or DFRF.

NSRDC	Naval Ship Research and Development Center
PT	Pressure Tunnel, Ames Research Center, Moffett Field, CA
RAE	Royal Aeronautical Establishment
SPT	Supersonic Pressure Tunnel, Ames Research Center, Moffett Field, CA
SUPWT	Supersonic Unitary Plan Wind Tunnel, Langley Research Center, Hampton, VA
SWT	Supersonic Wind Tunnel
T	tunnel
TDT	Transonic Dynamics Tunnel, Langley Research Center, Hampton, VA
TPT	Transonic Pressure Tunnel, Langley Research Center, Hampton, VA
TT	Transonic Tunnel, Langley Research Center, Hampton, VA
TWT	Transonic Wind Tunnel, Ames Research Center, Moffett Field, CA
UPWT	Unitary Plan Wind Tunnel, Langley Research Center, Hampton, VA
VKF	Von Kármán Facility, Tullahoma, TN

Symbols

A	aspect ratio or cross-section area (depending on context)
A_s, B_s, C_s	selected signals associated with DFWB control system
a_n	normal acceleration, load factor
a_t	transverse acceleration, also known as lateral acceleration
a_y	transverse acceleration, also known as lateral acceleration
C_D	drag coefficient, D/qS, except for figure 20
C_{D_0}	drag coefficient at zero lift
C_{D_b}	base drag coefficient
C_f	local turbulent friction coefficient, compressible
$\bar{C}_f$	local turbulent friction coefficient transformed to incompressible conditions
C_L	lift coefficient, L/qS
C_{N_A}	normal force coefficient, N/qS
C_p, b	base pressure coefficient
c	chord length of wing section
D	drag
d	diameter
g	acceleration of gravity
h	altitude
I_x, I_y, I_z	aircraft moment of inertia about axis indicated by subscript
i_t	horizontal stabilizer incidence angle, positive for trailing-edge down, deg

L	lift
L_A	aerodynamic component of structural load
L_T	thermal component of structural load
L_V	shear load on vertical tail, lb
L_{YJ}	rolling moment due to yaw jets, ft-lb
l	length
M	Mach number
M_e	Mach number based on boundary-layer edge conditions
$\boldsymbol{M}_j$	Mach number of the jet
N	normal force
P	static pressure
p	rolling angular velocity, deg/sec or rad/sec (fig. 5)
q	dynamic pressure, freestream, 0.7 M^2P
q_c	impact pressure
q_e	dynamic pressure at edge of boundary layer
$\sqrt{\overline{P}_s'^{\,2}}$	average static root-mean-square pressure fluctuation amplitude
R	Reynolds number
R_T	transition Reynolds number based on surface length on cone to transition
$\overline{R}_x$	Reynolds number based upon flow length x, transformed to incompressible conditions
R_x	Reynolds number based upon flow length x
r	yawing angular velocity, deg/sec
St	local Stanton number
s	Reynolds analogy factor, $s = \dfrac{2St}{C_f}$
T_R	boundary-layer recovery temperature, °R
T_{ad}	adiabatic temperature, °R
T_t	total or stagnation temperature, °R
T_w	wall temperature, °R
T'	T prime or reference temperature, °R
t	maximum thickness of wing section
t/c	maximum thickness-to-chord ratio of wing section
U_∞ or V	freestream velocity
α	angle of attack, deg
β	angle of sideslip, deg
ΔC_D	transonic wave drag increment
ΔM	incremental change in Mach number

ΔPLA	incremental change in throttle (power lever angle)
Δh	incremental change in altitude
$\Delta\delta_e$	incremental change in elevator angle, deg
δ_{a_t}	total aileron deflection, left aileron deflection minus right aileron deflection (positive for right roll) (left aileron deflection and right aileron deflection are each positive for trailing-edge down)
δ_e	elevator angle, positive for trailing-edge down, deg
δ_r	rudder deflection, positive for trailing-edge right, deg
ν_∞	kinematic viscosity for freestream conditions
ϕ	angle of bank, deg

Sign Convention

The important parameters that define aircraft attitudes and angular rates are referenced to a right-hand axis system with origin at the vehicle center of gravity. Positive directions are: forward (*X* axis), out the right wing (*Y* axis), and down (*Z* axis). All attitudes and angular rates are positive in a clockwise rotation about the appropriate axis as viewed in a positive direction. Angle of attack is positive when the *X* body axis is above the velocity vector. Angle of sideslip is positive when the *X* body axis is to the left of the velocity vector.

Abbreviations

a/c	aircraft
deg	degree
ft	feet
horiz	horizontal
kts	knots
lb	pound
m	meter
min	minute or minimum, depending on context
lb/ft^2	pounds per square foot
PLA	power lever angle
rad	radian
sec	second
sq	square
TE	trailing edge
WS	wing station

INTRODUCTION

Within the international community of aeronautical–transportation specialists there are important issues that require careful study before commitment to a high-speed air transport concept can be made. These issues include speed, range, seat capacity, propulsion concepts, and the effect on the environment, as well as materials, structures, stability and control, safety, and operational concerns.

With these and other related issues in mind, the European Symposium on Future Supersonic–Hypersonic Transportation Systems was held in Strasbourg, France in November, 1989. This symposium was organized by L'Académie Nationale de l'Air et del l'Espace (A.N.A.E., Fr.) and Deutsche Gesellschaft für Luft und Raumfart (D.G.L.R., Ge.) with the participation of the Royal Aeronautical Society (R.Ae.S., U.K.). Technical presentations were given by members of these societies and by participants from other European nations as well as by American and Japanese specialists.

More than 40 presentations were given during the 2 1/2-day symposium including 2 papers representing the flight experience and proposed activities of the NASA Dryden Flight Research Facility. These two presentations, "The Need for a Hypersonic Demonstrator" and "NACA—NASA Supersonic Flight Research" were delivered by Mr. Theodore G. Ayers, then Deputy Director of the Dryden Flight Research Facility (DFRF). The two DFRF presentations are represented in print in reference 1, which is an edited compilation of the proceedings of the previously mentioned symposium.

In reference 1, the NASA DFRF presentations are printed without references which somewhat diminishes their usefulness and deprives the reader–researcher of interesting historical and background information. In addition, the Supersonic paper is printed from a transcription of the tape recording taken during the symposium. Thus the rendition given in reference 1 is in the first person and in a predominantly oral format. For the reasons cited, and because a wider distribution of the Supersonic paper is considered appropriate, this expanded document has been prepared.

The NASA DFRF evolved through several agency reorganizations beginning in 1946. The original organization was the Muroc Flight Test Unit of the National Advisory Committee for Aeronautics (NACA).* The Muroc Flight Test Unit began as a small group of engineers and technicians from the NACA Langley Aeronautical Laboratory who were transferred to the Muroc Army Air Field in California's Mojave Desert in 1946.[2] The NACA Muroc Flight Test Unit was formed to provide technical guidance for testing the Army/Bell XS-1 rocket aircraft (later known as the X-1). The X-1 was to become the first manned airplane to exceed the speed of sound on October 14, 1947.

This report begins with the early X-1 series of research aircraft, and provides selected examples of supersonic flight research from the next four decades. This document begins with the transonic—supersonic demonstration and evaluation of the adjustable horizontal stabilizer on the X-1 airplane. Twelve other examples of supersonic flight research follow, which include aircraft efficiency, stability and control, structural loads, model-to-flight correlation, parameter estimation, and more recent developments leading to the integration of flight and propulsion controls and digital fly-by-wire technology.

*Later names for the organization were, in order, High-Speed Flight Research Station, High-Speed Flight Station, Flight Research Center, Dryden Flight Research Center, and the Dryden Flight Research Facility. On March 1, 1994 the organization was reestablished as the Dryden Flight Research Center.

As the title of this report indicates, the research described herein was either obtained at supersonic speeds or enabled subsequent aircraft to penetrate or traverse the supersonic region. Consequently, this report does not address significant flight research accomplished at subsonic speeds or at hypersonic speeds.*

While the types of aircraft in this report vary widely, and a broad range of aeronautical disciplines are discussed, many NASA-DFRF aircraft–programs are not included. The 13 examples presented are categorized into 3 specific stages of aeronautical flight research and were chosen to show that flight research has evolved through several stages since the post World War 2 years. The three stages which represent the DFRF supersonic flight research experience are

Stage 1 Barriers to Supersonic Flight

Stage 2 Correlation—Integration of Ground Facility Data and Flight Data

Stage 3 Integration of Disciplines

The relevance of each stage of aeronautical research and the 13 examples will be highlighted in a summary following each stage in the Discussion and in the Concluding Remarks section. The table on page 58 lists the 13 selected examples of supersonic flight research in relation to the 3 research stages. In the meantime, the authors hope that the aircraft types, the aeronautical disciplines, and the solutions to problems presented herein will reveal the significance of exposing the problems of existing airplanes and the advance design concepts of future aircraft to the realities of the flight environment. Because, to quote Dr. Hugh L. Dryden, the purpose of full-scale flight research is "… to separate the real from the imagined … to make known the overlooked and the unexpected problems."

DISCUSSION

Stage 1: Barriers to Supersonic Flight

Initially the most obvious of the barriers to achieving supersonic flight were the rapid changes in control effectiveness and the sudden onset of wave drag near Mach 1. Though the first manned flight to exceed sonic speed did not by itself solve the problems associated with these barriers, it demonstrated that their ultimate solution was likely. As indicated in the introduction, that first flight to exceed the speed of sound was made by the X-1-1 on October 14, 1947.[2]

The first two X-1 airplanes had the same fuselage and planform configurations, but the thicknesses of the wings and horizontal stabilizers were different. Before the design was finalized there were two opposing philosophies regarding wing thickness. One group wanted a maximum thickness of 12 percent of chord. That way, detailed pressure data could be obtained for supercritical flow at an aircraft Mach number significantly below one and such a wing would be stronger than a thin wing. The other faction wanted a maximum thickness of 5 percent of chord so as to penetrate deeply into the supercritical region

*The definition of hypersonic, as applied to this report, is $M \geq 5.0$. Thus supersonic will refer to Mach numbers from 1.0 to less than 5.0.

with lower shock strength (thus attenuating transonic nonlinearities); perhaps even permitting supersonic flight.[3] A compromise was reached which resulted in the following thicknesses.

Aircraft	*t/c* for wing, percent	*t/c* for horizontal stabilizer, percent
X-1-1	8	6
X-1-2	10	8

For a specific airplane, the thickness of the horizontal stabilizer was less than for the respective wing at the insistence of NACA advisors. This was so that the stabilizers would not experience transonic (shock-stall) problems simultaneously with the respective wing.

Not surprisingly, it was the X-1 airplane having the thinner wing that first flew supersonic. This airplane is shown in figure 1 along with a reproduction of the recording traces of the first “Mach jump.” Note also the Mach diamond pattern in the rocket exhaust. The upper trace showing the jump is a history of impact pressure (q_c) i.e., the difference between the stagnation pressure sensed at the tip of the noseboom head and the static pressure sensed from flush orifices. The flush orifices were located several inches behind the tip of the noseboom head and the static pressure sensed is shown as the lower trace, labeled 5H. The time scale is indicated by the numbers beginning at 145 sec with time advancing to the right.

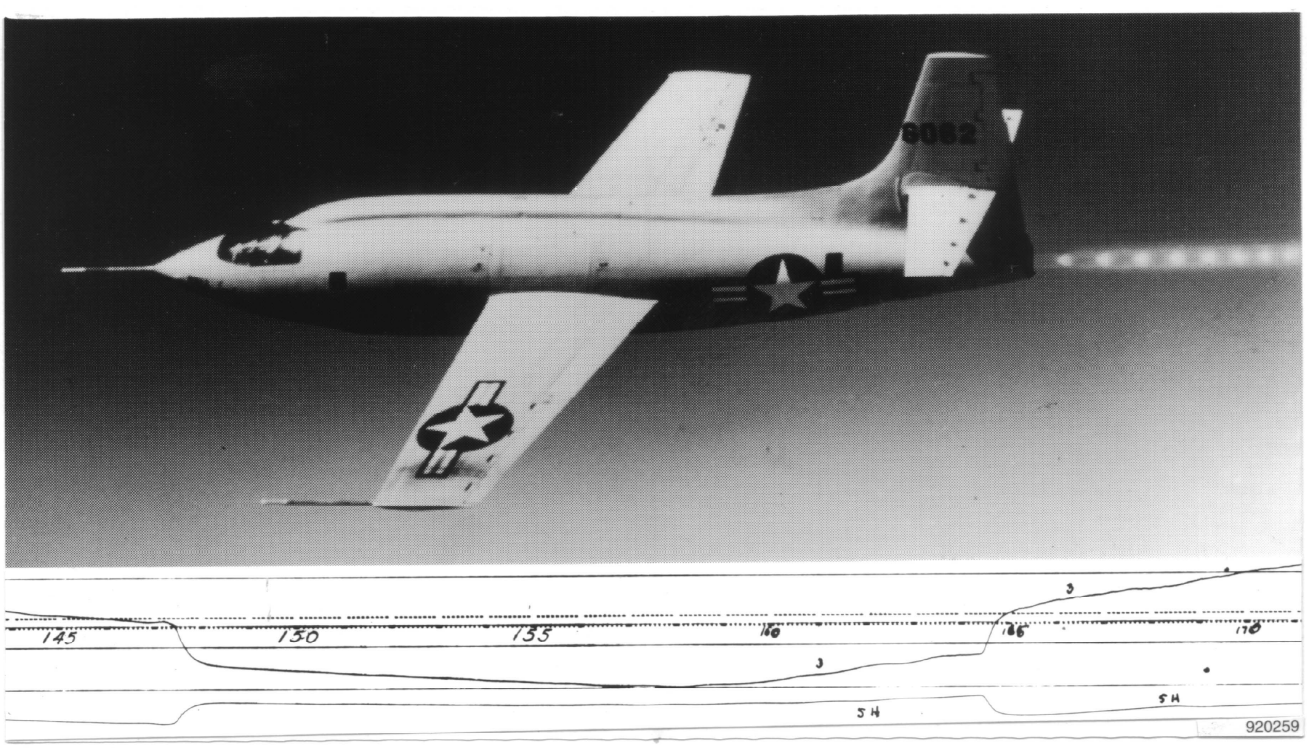

Figure 1. Historic first recorded Mach jump, XS-1, October 14, 1947.

The first jump was caused as the primary bow shock wave generated by the fuselage nose passed over the flush orifices at about 147 sec. As the airplane decelerated the bow shock passed over the flush orifices again in the opposite direction at about 164 sec. Though the recorded jump interval was about 17 sec, the airplane was actually slightly supersonic for 20.5 sec when an accounting was made for the effects of compressibility on the measured static pressure. The maximum Mach number reached during this flight was 1.06.

This airplane was to reach higher Mach numbers during later flights, though it never ventured far into the supersonic region because of its limited fuel capacity. Nevertheless, this airplane and its sister craft, the X-1-2, contributed significantly to all subsequent aircraft which performed either within or beyond the transonic speed region. A compilation of early research from the X-1-1 and the thicker winged X-1-2 is found in reference 4.

Figure 2 shows the relationship of the maximum Mach numbers obtainable for the early rocket-propelled research aircraft to the Mach capability of contemporary fighter aircraft over a period of about one decade.[2] The lead time for the research aircraft shown was approximately 5 years. This lead was established not only by the earliest X-1 airplanes but by other follow-on research aircraft. The lead in years demonstrated by these unique high-performance research aircraft illustrates how knowledge and concepts developed through such facilities provided the basis and confidence for increasing Mach capability of subsequent operational military aircraft.

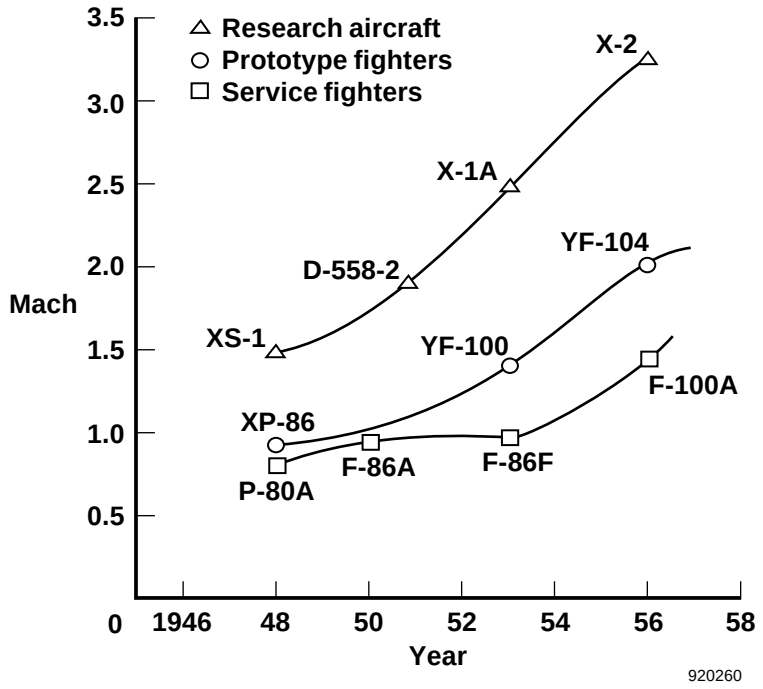

Figure 2. Leader-follower relationship between research aircraft, military fighter prototypes, and military fighters in service, reference 2.

Though these unique high-performance research aircraft extended the energy boundaries of achievable Mach number and altitude, more conventional aircraft are also important to conduct flight research. Modified, highly instrumented, operational aircraft are often used to fill in significant details to the technical fabric of aeronautical knowledge. It will become evident that both kinds of aircraft (unique specially built and modified-operational) are required to fulfill the purpose of flight research as defined earlier by Dr. H.L. Dryden, page 6.

The Adjustable "All-Movable" Stabilizer —It was apparent after World War 2 that to fly supersonically, airplanes would have to maintain control through regions characterized by rapid trim changes and diminished control effectiveness. Consequently the X-1 airplanes and the follow-on X-2 [5] were provided with an in-flight, adjustable (all-movable) horizontal stabilizer, at the insistence of NACA, to compensate for the anticipated loss in elevator effectiveness. The earliest versions of the tiny X-1 airplanes did not have room for auxiliary power sources to operate a hydraulic system. Therefore, this pioneering transonic adjustable stabilizer had to be actuated by other means. The initial approach used a 24-volt battery-powered electric motor to drive a screw jack which changed the stabilizer incidence angle. Following a few low-speed glide flights it was decided that faster rates of change in incidence angle were needed. Consequently pneumatic motors were placed at each end of the screw jack, and these provided rates that were adequate for the transient conditions that would be encountered during powered flight. These pneumatic motors were driven by gaseous nitrogen. [6,7] Gaseous nitrogen at various pressure levels was also used to lower the landing gear, operate the flaps, deliver propellants to the rocket motor, operate the gyros, and pressurize the cockpit.

An example of data showing the benefits of the movable stabilizer is shown in figure 3. The left portion of figure 3 shows trim curves obtained at various horizontal stabilizer settings (i_t) for the X-1-2, corrected to a constant normal force coefficient of 0.3.[8] The data show that for stabilizer settings near 1° the airplane could be trimmed by the elevator (δ_e) through the speed range of Mach numbers above 1.0. However, if the stabilizer is set at 2°, there is insufficient up-elevator for control of the "tuck";* and at a setting of 0.5° there is too little down-elevator to overcome the nose-up trim change. The trim curve for the stabilizer, with $\delta_e = 0°$, is shown by the dashed line (where the ordinate scale applies).

The effectiveness of this control surface as a function of Mach number is shown in the right-hand portion of figure 3. These data together with other data, not shown, indicate that at Mach 1, the elevator was only 1/20 as effective as the stabilizer. Subsequently there resulted the general adoption of all-movable stabilizers on later high-speed airplanes … first the X-2, the X-3, and the F-86 with all-movable horizontal stabilizers and later the X-15 research airplane having horizontal and vertical stabilizers all-movable. Virtually all supersonic fighter-interceptors flying four decades later use the all-movable stabilizer concept as well as larger cruise aircraft which probe even slightly into the transonic region. Current and future supersonic and hypersonic aircraft, manned or drone, also must rely on all-movable stabilizers; a concept which was first evaluated in transonic—supersonic flight in the late 1940's.

*Tuck as used here was the tendency for the nose of an airplane to rotate downward in pitch.

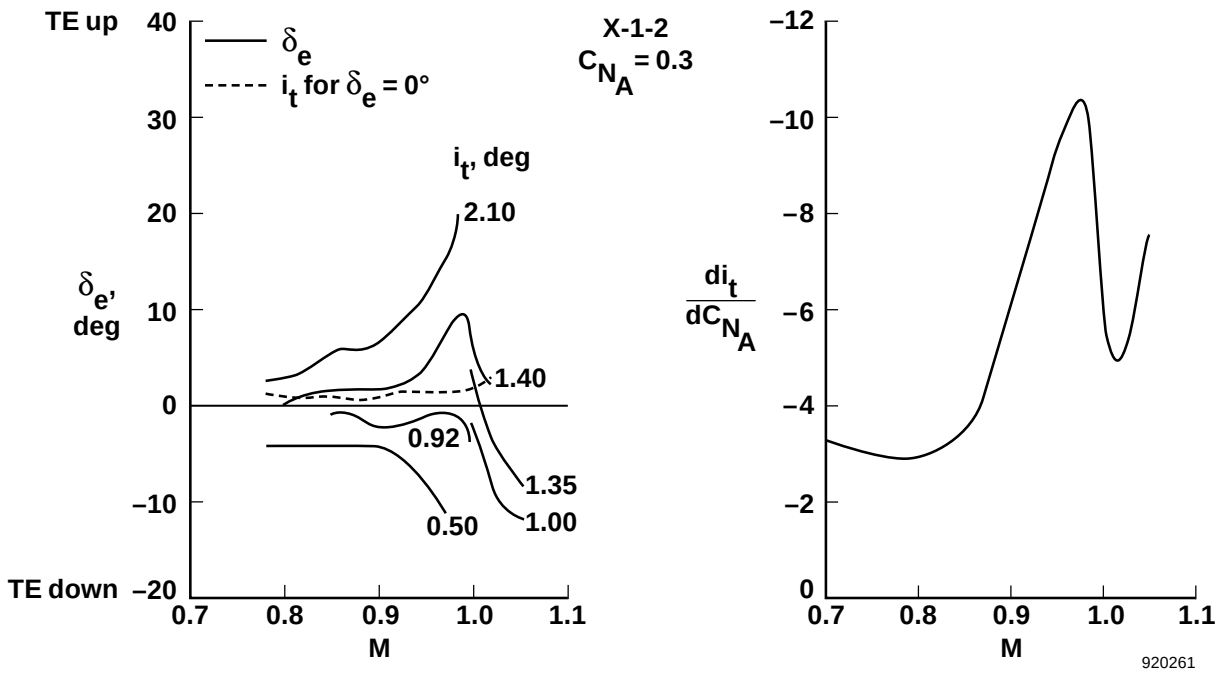

Figure 3. Elevator trim and stabilizer effectiveness, X-1 #2.

The Identification of Inertial Coupling—In the late summer of 1954 the NACA flight research facility, then called the High-Speed Flight Station, began flying another of the experimental "X" series of airplanes, the long slender X-3 (fig. 4). The X-3 was designed for a sustained Mach number of at least 2 and was to be used to evaluate the flight characteristics of unswept, thin, low-aspect ratio wings. Though the X-3 was shaped for Mach-2 flight, it required a gradual diving maneuver to reach even M = 1.2 because it never received the higher rated thrust turbojet engines that were originally intended for it.

Like supersonic aircraft soon to follow, the X-3 had geometric and mass distribution characteristics that made it prone to inertial roll-pitch coupling, that is, the wing was thin and of low-aspect ratio and most of the vehicle mass was concentrated about the longitudinal (X) axis (see aspect ratio and inertia ratios in fig. 4). This resulted in small rolling moments of inertia as compared to the pitching and yawing moments of inertia. In addition, the high empennage and low, long nose contributed to a high roll-yaw cross product of inertia, and directional stability was compromised by the long nose of relatively large side area.

Thus when the X-3, with this combination of physical characteristics, was exposed to rapid lateral maneuvering, violent inertial coupling was encountered. Analysis of the X-3 data led to an understanding of the inertial coupling problem that destroyed a series of contemporary supersonic aircraft during the early and mid-1950's.[2,5] Less destructive encounters that led to increased understanding of inertial coupling and related analog studies are reported in references 8 through 12.

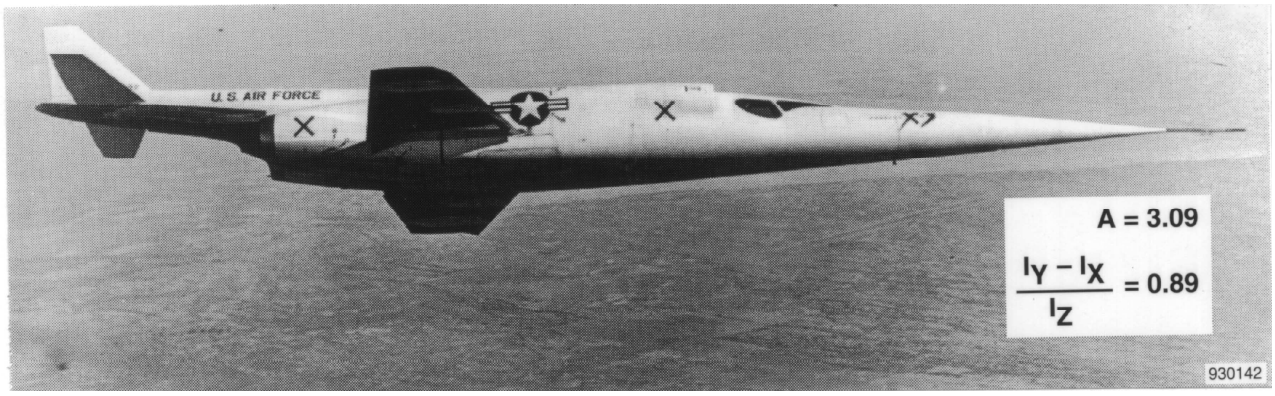

Figure 4. The X-3 airplane and physical characteristics which contribute to inertial coupling.

In the case involving the X-3, it was during a handling qualities investigation consisting of abrupt aileron rolls (with rudder fixed, from a wings-level attitude) that a violent coupled lateral—directional oscillation occurred. The left part of figure 5 shows favorable sideslip built up with rolling velocity in response to the aileron deflection. Angle of attack did not vary greatly until a sideslip angle of almost 20° was reached (time ≈ 4.0 sec), at which time angle of attack decreased rapidly to –13°. The pilot applied up-stabilizer to stop the pitch-down tendency which may have contributed to the 19°-angle of attack when the airplane then pitched up. When the rolling motion stopped, the airplane quickly recovered.

The violence of this maneuver can be understood best by noting (on the right portion of fig. 5) that the load factor changed from –6.7 *g* to +7.0 *g* within a 0.5-sec interval. Note the relationship of these levels to the dashed horizontal lines representing the design limits for load factor. Note also that the transverse, or lateral, acceleration measured was very close to the design value and the vertical stabilizer shear loads reached approximately 56 percent of the design level.

Though the X-3 was not the first airplane to experience inertial coupling, see for example references 2 and 13, it served as the prototype encounter with inertial coupling to demonstrate the phenomenon unadulterated by extraneous circumstances such as propulsion factors. The X-3 occurrence was recognized by NACA flight research engineers as a striking example of coupling problems. These problems were foreseen theoretically by William H. Phillips of the Langley Aeronautical Laboratory a few years earlier for supersonic configurations having short wing spans and a highly loaded fuselage.[14]

The timely recognition of the X-3 occurrence as potentially inherent in many supersonic aircraft resulted in quick corrective measures for the F-100 fighter,[15,16] the F-104, and other supersonic airplanes, either in configurational, control system design, or operational changes. Current fighter-interceptor airplanes, in the United States and elsewhere, now have improved aerodynamic configurations which show in some recognizable ways influence from the understanding of inertial coupling obtained in the 1950's. In addition, automatic flight-control systems of highly maneuverable airplanes now incorporate feedback compensation to minimize the effects of coupling.

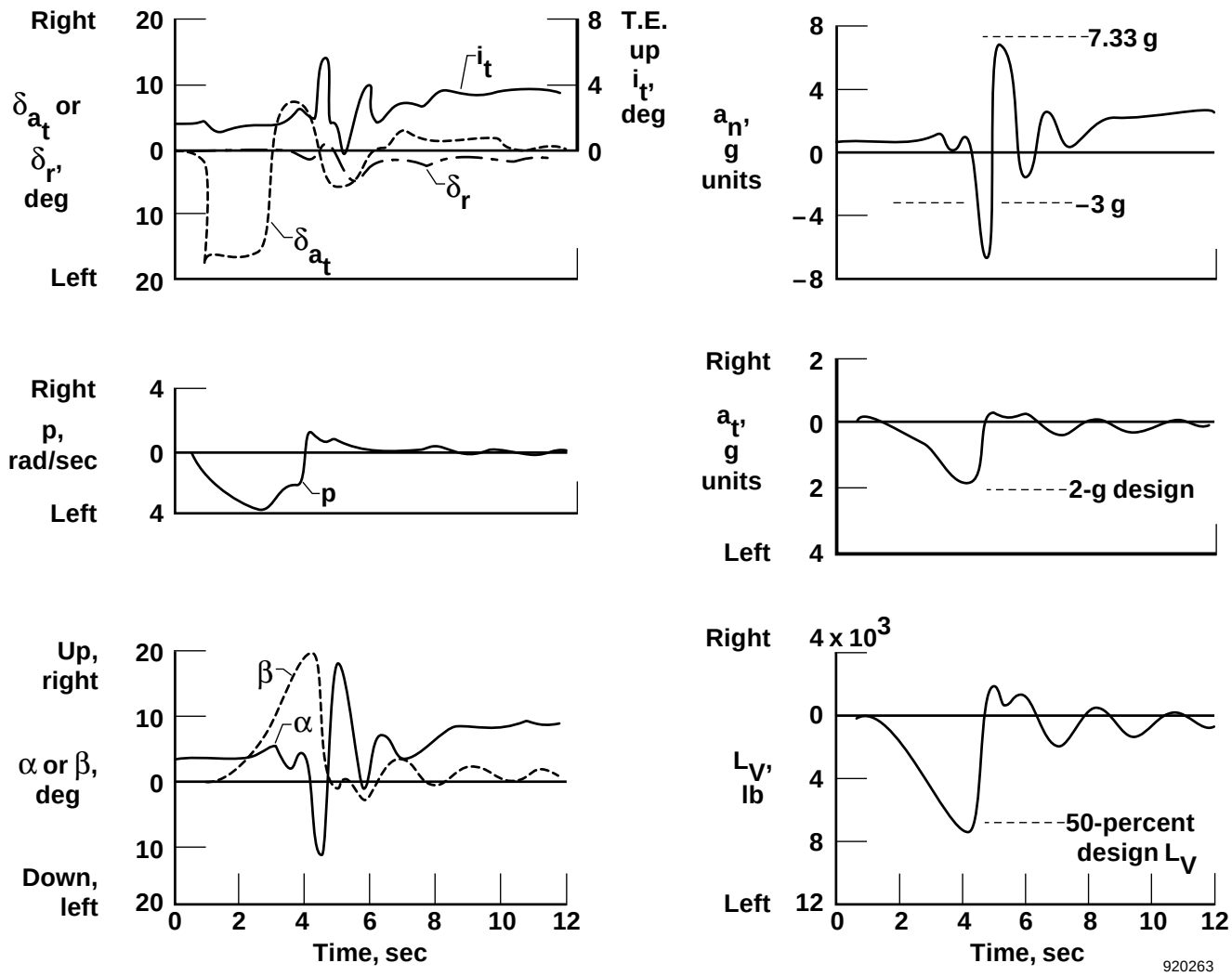

Figure 5. Flight data obtained while the X-3 airplane was performing an abrupt aileron roll, $M = 1.05$, $h \sim 30,000$ ft.

The Area Rule: Reducing the Magnitude of the Wave-Drag Barrier—There was experiential evidence of the transonic drag-rise long before and during the World War 2 years. Though pre-World War 2 aircraft were not even able to achieve sonic flow over the wings, the performance of propellers was impaired because of shock wave losses as propeller tip speeds resulted in critical local Mach numbers. During World War 2 ever larger engines and propellers resulted in level flight speeds of more than 400 mph for a few fighter aircraft. In diving flight these aircraft sometimes experienced local sonic flow over portions of the wings which resulted in flow separation, greatly increased drag, and occasional loss of control.

These experiences, the earlier propeller tip shock experience, and model data provided ample warning of the formidable drag-rise barrier that future operational aircraft would encounter as they tried to pass through the speed of sound. Though the X-1 airplane exceeded sonic speed soon after the war (October 1947), these airplanes were air launched from a “mother” airplane and they used most of their

fuel to overcome the wave-drag barrier. Clearly, a reduction of wave drag was needed for more conventional turbojet powered aircraft to routinely fly supersonic.

Meanwhile, in wind-tunnel testing attempted at transonic speeds, the effects of compressibility, wall interference, and tunnel choking were barriers that confounded attempts to understand and reduce wave drag. Therefore, an intense effort was launched during the 1940's at the NACA Langley Aeronautical Laboratory which ultimately resulted in the development of the slotted throat concept.[17,18] By late 1950 the multislot configuration for the 8-ft throat was ready for research usage. This modification was of extreme importance in that reasonably uniform, choke-free flow could now be obtained throughout most of the transonic speed range (that is, up to $M = 1.14$). Stated in more meaningful terms, fundamental aerodynamic concepts could now be studied in the wind tunnel through much of the transonic region, and wave drag would be one of the targets of new research.

During the following year (1951) Dr. Richard T. Whitcomb and his coworkers used the modified (multislotted) 8-ft tunnel as a research tool for developing a revolutionary concept to reduce the transonic drag rise (wave drag) of supersonic aircraft. The concept was based on the premise that "near the speed of sound the zero-lift drag rise of a wing-body configuration generally should be primarily dependent on the axial development of the cross-section areas normal to the airstream."[19,20] The data supporting this principle showed that the transonic drag increment (i.e., the wave-drag increment) was virtually the same for a wing-body combination as for a body alone which had the same cross-sectional area development, that is, an equivalent body. This is demonstrated in the bottom portion of figure 6 from reference 19.

Because it was obvious that bodies with a smooth streamline area development had the lower wave-drag increments, it was natural to use the same principle for real aircraft (that is, for bodies plus lifting surfaces) to produce a configuration with a smooth, overall cross-sectional development. This was done by reducing surface slopes which contribute to cross-sectional area growth and decay, and using judicious lengthening, indenting, and in some cases, volume addition.

An early application of this process, popularly known as the area rule, was the F-102 airplane. The prototype of this airplane, which needed reduced wave drag, is shown on the right-hand side of figure 7. The left side of figure 7 shows the modified airplane, the F-102A, which was reshaped with fuselage indenting, lengthening, and volume addition. Also shown are the corresponding cross-sectional area development curves for each full-scale configuration.

The lower portion of figure 7 shows the wave drag increments as a function of Mach number for the full-scale aircraft, and corresponding pairs of data from 1/5-scale rocket-launched models, 1/20-scale wind-tunnel models, and 1/60-scale equivalent bodies.[21*] Taken together, these data verified the effectiveness of the area smoothing process and the adequacy of the equivalent body concept toward the wave-drag sub-scale simulation for a complete wing-body configuration. This flight program (YF-102 and F-102A) not only provided verification of the important area rule, but also established the modified

[*]The relatively smaller wave-drag difference for the 1/5-scale models is believed to be caused by smaller differences in the afterbody geometry for this pair of models as compared to the other configuration pairs.

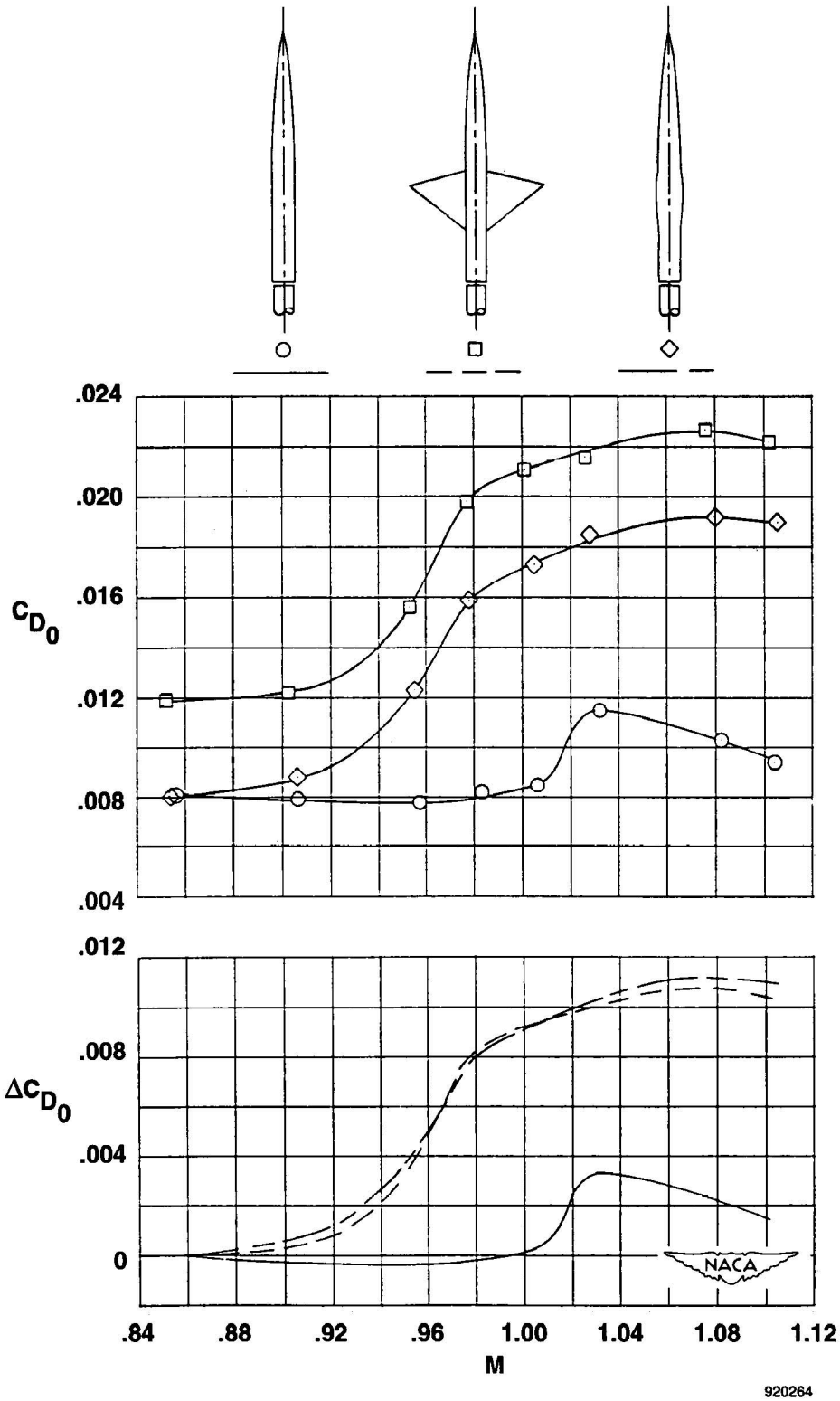

Figure 6. Comparisons of the drag rise for unswept-wing and cylindrical-body combination with that for the comparable (equivalent) body of revolution and the cylindrical body alone, reference 19.

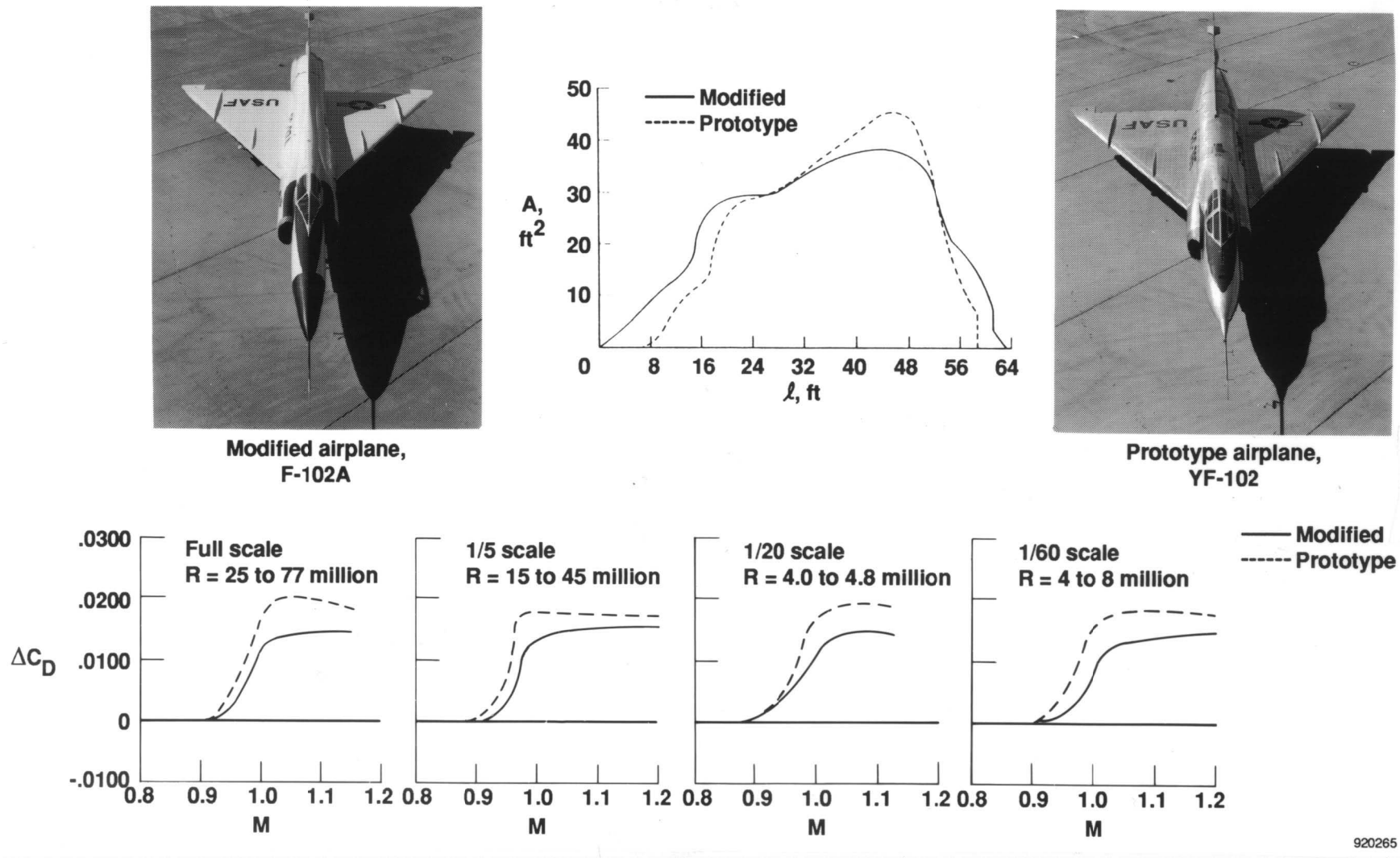

Figure 7. Transonic drag-rise (wave drag) characteristics of the F-102 aircraft with and without area-rule modifications.

8-ft wind tunnel with the slotted test section as a credible transonic research facility. This same tunnel would later be the lead facility in the development of the supercritical wing (SCW) and winglets.

The area-rule concept became a standard means of reducing wave drag for supersonic aircraft. Consequently, supersonic aircraft designed and built nearly four decades later possess smaller wave-drag increments, which allow these airplanes to traverse the "one time" sonic barrier with less fuel consumption than would otherwise be required. Reference 22 describes an extension of the transonic area rule (that is, the supersonic area rule) which is more often applied to the supersonic aircraft of the last three decades.

Reaction Controls: The Problem of Control at Low Dynamic Pressure—During the mid-1950's, after the speed of sound had been exceeded, then doubled by the D-558-Phase II airplane and increased again to Mach 3.2 by the X-2; the problem of maintaining aerodynamic control at the low dynamic pressures associated with flight at high altitude ($q \leq 20$ lb/ft^2) became real. In addition, because the development of larger rocket engines was a virtual certainty, travel to near-orbital and orbital velocities was anticipated within, perhaps, the next two decades. Consequently, it was natural to investigate alternative means of aircraft control for the low dynamic pressure conditions where aerodynamic controls would be insufficient (or completely absent for orbital considerations).

Though it is primarily orbital, suborbital, and hypersonic vehicles that require reaction control capability, it was recognized in the mid-to-late 1950's that the earliest flight evaluation of reaction controls would occur with supersonic research aircraft. It was also believed that the flight research should be preceded by ground-based simulation studies.

The pioneering jet reaction (reaction control) simulation work at Dryden's parent facility, NACA's High-Speed Flight Station, spanned the last years of the NACA organization and the first NASA years. A two-phase study was begun; one was a fixed-base setup with an analog computer to solve the equations of motion and the other used a three-degree-of-freedom mechanical simulator wherein the pilot experienced motions.[23]

The analog computer simulator represented the airplane in five-degrees-of-freedom with control provided from the pilot's short control stick, as shown on the left side of figure 8. The stick was unconventional for its time because it was necessary for the pilot to control about three axes through one control device. The stick pivoted fore, aft, and laterally for pitch and roll control, and lateral thumb movement provided yaw control. For most of the study, the pilot presentation consisted of an oscilloscope trace for pitch and bank angle, and the simple volt meter, below, for angle of sideslip seen on the right side of figure 8.

The mechanical simulation was achieved through the device shown in figure 9. It was referred to as the "iron cross" and had a mass distribution which matched the inertia ratios of the X-1B airplane. The X-1B was expected to be the first airplane to demonstrate jet reaction controls in an actual low dynamic pressure environment.[24,25,26] A universal joint from a truck permitted motion about three axes. High-pressure nitrogen gas was expanded selectively through the six jet nozzles to provide the reaction forces. Standard NACA flight-type recorders were used to record control stick position and the various angular rates. Short pulse (i.e., on-off) control inputs were used, as had been developed as a part of the earlier analog computer study.

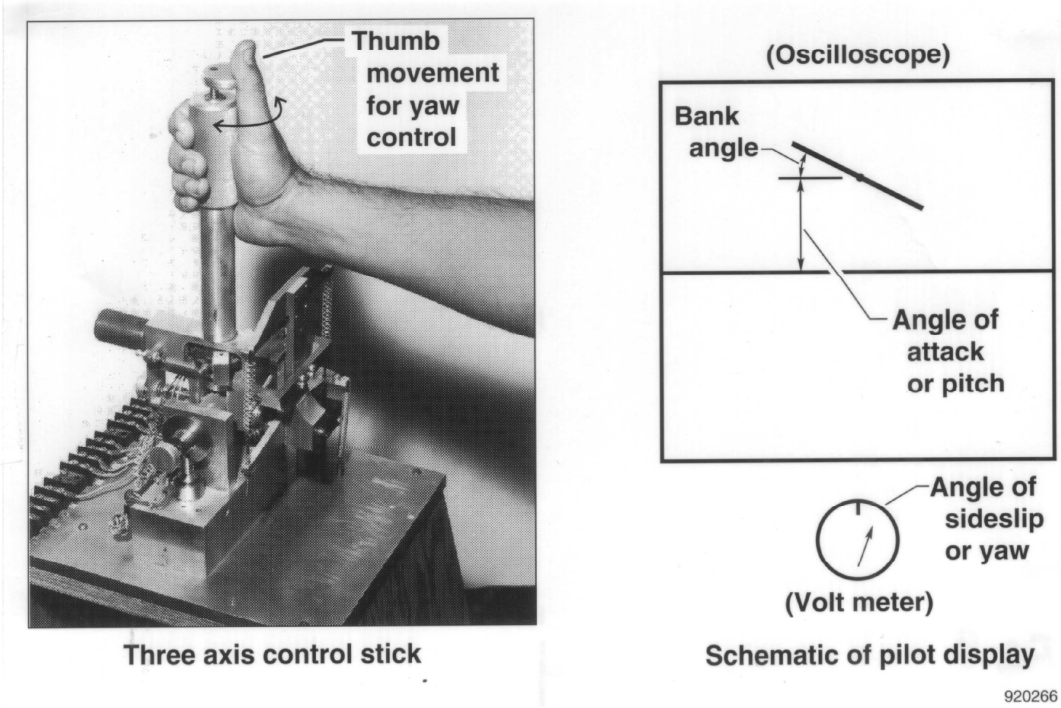

Figure 8. Analog control stick device and display.

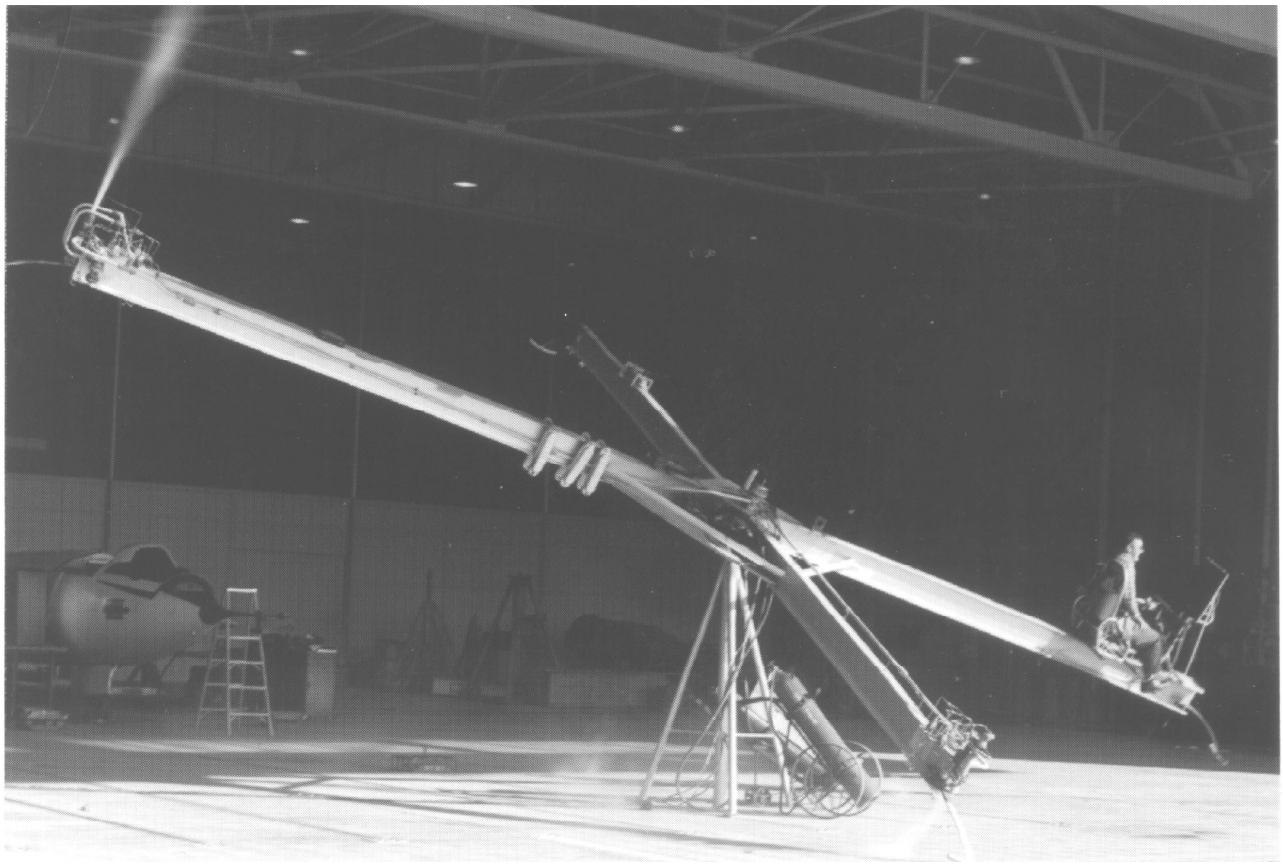

Figure 9. Mechanical reaction control simulator, iron cross

These two simulation methods, analog computer and mechanical iron cross, showed that

- control techniques were somewhat different than with aerodynamic controls,
- perfectly trimmed flight would be difficult to maintain manually,
- it was very easy to over control, and
- no conclusive difference was established between ease of control with full-on, full-off controls and proportional jet controls, but it was noted that the pilots used the proportional controls as on-off (or bang-bang) even when they had proportional controls, and a required dead-band was included in the proportional control system.

Now it was time for a demonstration in flight.

As it turned out, the X-1B could not be used as had been planned because it developed fatigue cracks in the propellant tank and was retired from flight status. Subsequently a hydrogen-peroxide reaction-control system was designed for an F-104 airplane.[27] Though the F-104 could not ordinarily achieve flight at the altitudes required for low dynamic pressures, by using a pull-up "ZOOM" maneuver following a level flight acceleration to $M = 2$ at about 40,000 ft (12,000 m) of altitude, relatively low dynamic pressures were reached.* The left side of figure 10 shows the F-104 with the reaction controls installed. Note the nozzles in the fuselage nose and the wingtip pods that housed the roll nozzles. The right side of figure 10 shows dynamic pressures obtained on some of these flights. More than half of the flights provided dynamic pressure values below 20 lb/ft^2. This range of pressure could be maintained for approximately 30 sec.

From these flights it was learned that a reliable hydrogen-peroxide reaction-control system could provide control at low dynamic pressures for an airplane, and actual flight experience was obtained by several pilots. It was also determined that for a turbojet airplane such as the F-104, the control task was complicated by engine gyroscopic coupling that related aircraft pitching and yawing motions.

Taken together, the ground-based simulation studies and the F-104 flight experience provided design guidelines that were applied to the X-15 research airplane, which would routinely depend on jet reaction controls. As an added note of interest, the reaction-control "stick" used on the X-15 airplanes is shown in figure 11. The same short-pulse type of technique developed during the earliest studies was retained.

The lessons learned from the simulation studies and the F-104 and X-15 reaction control experiences have been applied to the follow-on manned space vehicles Mercury, Gemini, Apollo, and the Space Shuttle. This pioneering effort is a reminder that a research vehicle representing one speed region (in this case the supersonic region) may contribute significantly to a future class of vehicles which will fly in a different speed region, i.e., hypersonic velocities, or vehicles which will move through space.

*To reduce the risk to the pilot during repeated flight to high altitude, in case of failure of normal engine-bleed cockpit pressurization, an auxiliary cockpit pressurization system was designed and installed in the F-104. It used nitrogen as the pressurizing medium, the same as was used in the early X-1 airplanes which were designed in the mid-1940's. An inert gas was chosen to reduce the risk of cockpit fire.

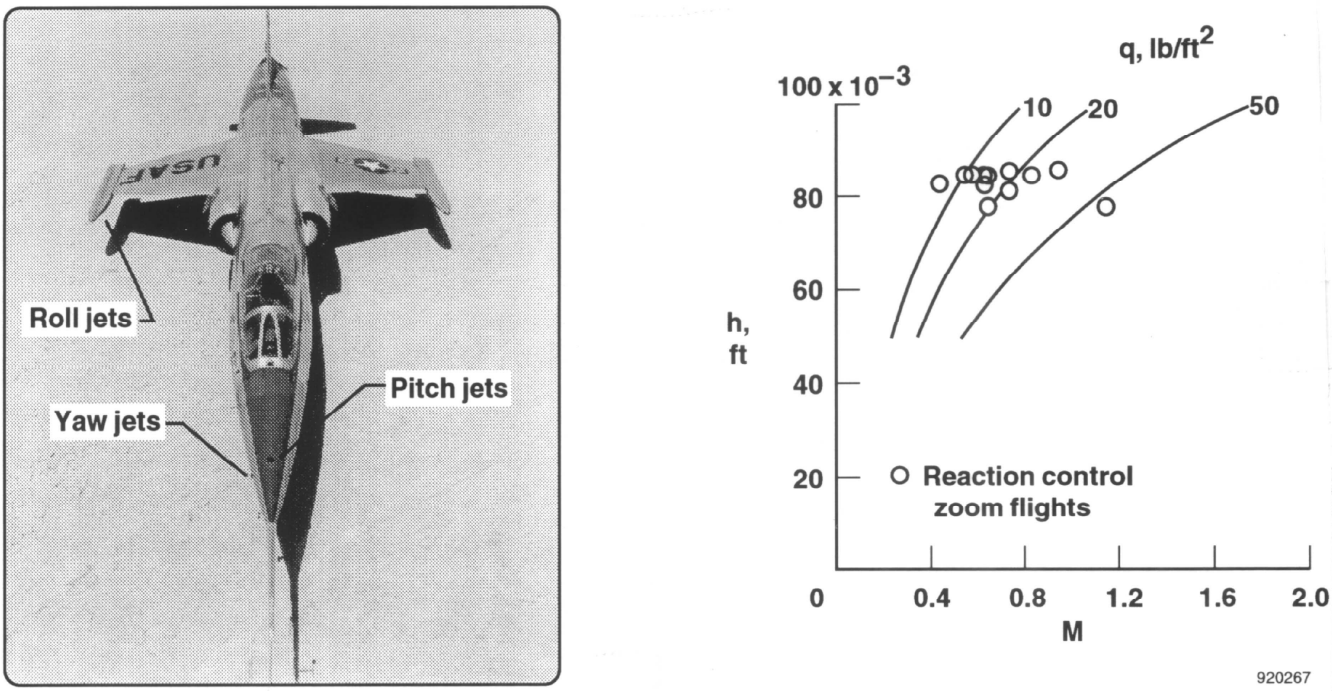

Figure 10. F-104 airplane with reaction control jets and flight conditions where reaction-control data were obtained.

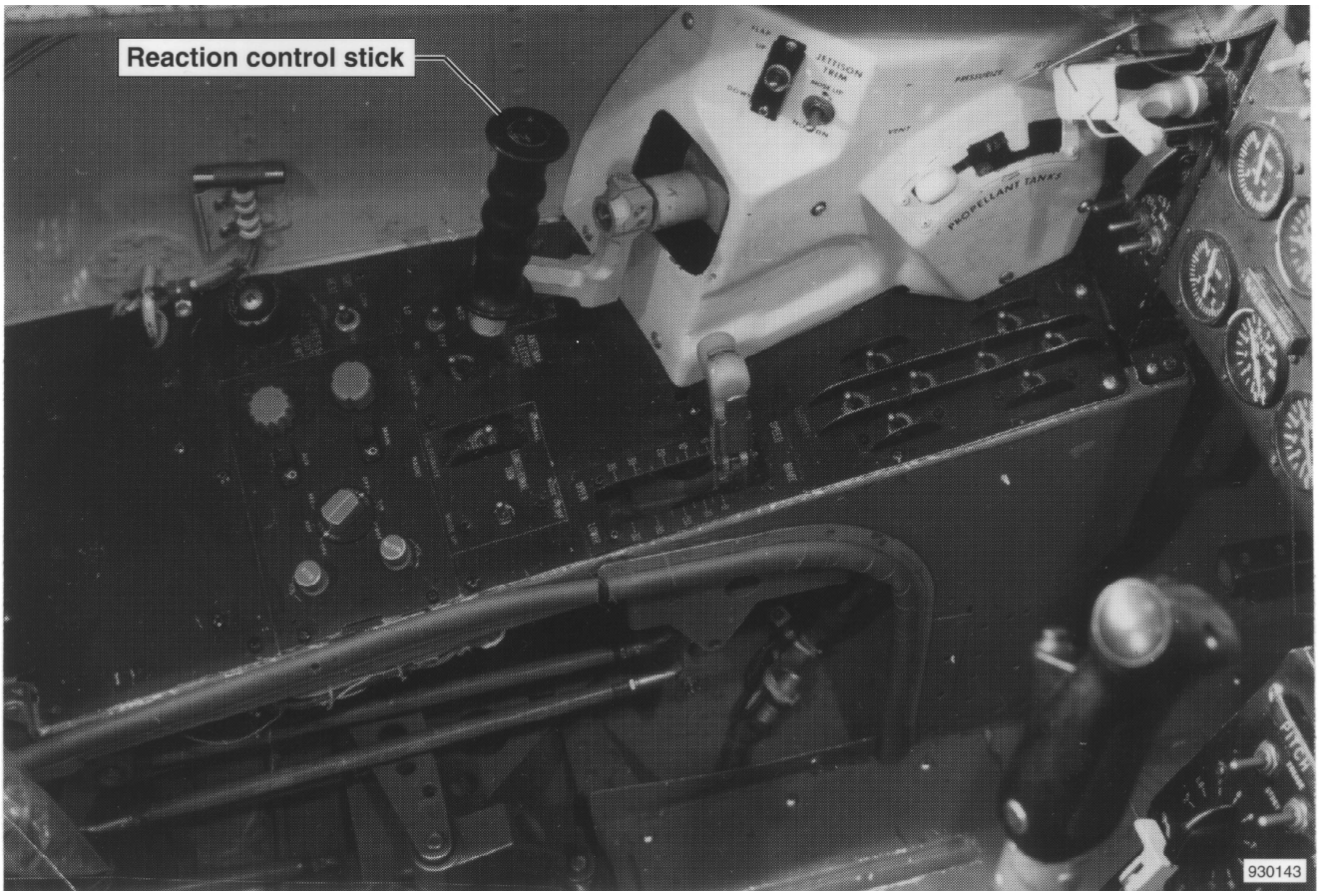

Figure 11. Reaction control stick device in X-15 cockpit.

Summary of Stage 1: Barriers to Supersonic Flight—A common characteristic of the four barrier issues is the lasting influence of each. The adjustable stabilizer, introduced on the X-1 series of aircraft and first flown (transonic and through Mach 1.0) in 1947, is used on all current high-performance aircraft and large transports - four decades later. In a related way, high-performance interceptor-type aircraft continue to have their planforms, the arrangement and sizing of stabilizing surfaces, and their cross-sectional area distributions configured according to the principles of the area rule and the lessons from the inertial coupling studies. The inertial coupling flight research also resulted in the use of feedback compensation in the automatic flight-control systems of current fighter-interceptor aircraft. Furthermore, the pioneering reaction-control research resulted in system design principles and short-pulse techniques which are still used for free-flight vehicles and aircraft for the entire range of speeds from vertical take-off and hovering through supersonic, hypersonic, and orbiting velocities. The application of the knowledge learned from these four research items will continue into the future as long as mankind flies aircraft and space vehicles.

Stage 2: Correlation–Integration of Ground Facility Data and Flight Data

As mentioned in the introduction, the supersonic flight research conducted at the NASA DFRF may be categorized in stages wherein needs and emphasis evolve in response to the quest for greater performance, efficiency, and safety. The next few experimental items (categorized as Stage 2) do not represent barriers that must be overcome to fly supersonically; but represent the process of refining research methods and understanding better the relationship of theory, ground facility data, and reality born from full-scale flight.

Supersonic Wind-Tunnel Model-to-Flight Drag Correlation—Walter C. Williams and Hubert M. Drake referred to the X-series research airplanes of the late 1940's and 1950's (fig. 12) when they wrote[8] "One of the important uses of the research data obtained in this program* has been the validation of the vented-throat transonic tunnels during their development by NACA." Looking ahead to the X-15 research aircraft (capable of supersonic–hypersonic speeds) they realized that in addition to exploring the operational and piloting aspects of near-space equivalent and entry flights, the X-15 would also provide data for evaluating–validating wind tunnels and theory for a new expanded range of flight speeds.

For the aeronautical engineer responsible for predicting the full-scale flight drag of supersonic aircraft from subscale model tests, the X-15 provided a unique opportunity. This was because the X-15 was capable of providing accurate drag data from flight as it was simple in shape and structurally rigid. In addition, because it was rocket powered, it had no air inlets and by obtaining the data during coasting flight, uncertainties associated with measuring thrust were avoided. Two views of the X-15 airplane are shown in figure 13.

The results of the correlation of 1/15-scale model data for the X-15 and the full-scale flight drag data are shown in figure 14 as a function of Reynolds number.[28,29] The model data are extrapolated to the full-scale Reynolds numbers using the Sommer and Short "*T*-prime" method[30,31] for a flat plate and a turbulent boundary layer.

*Williams and Drake were referring to the research obtained from the various (pre-X-15) "X series" research aircraft and the D-558-II and D-558-I aircraft.

Figure 12. Some of the research airplanes of the late 1940's and 1950's. Clockwise from lower left: X-1A, D-558 I, XF-92A, X-5, D-558 II, X4, and the X-3 in the center.

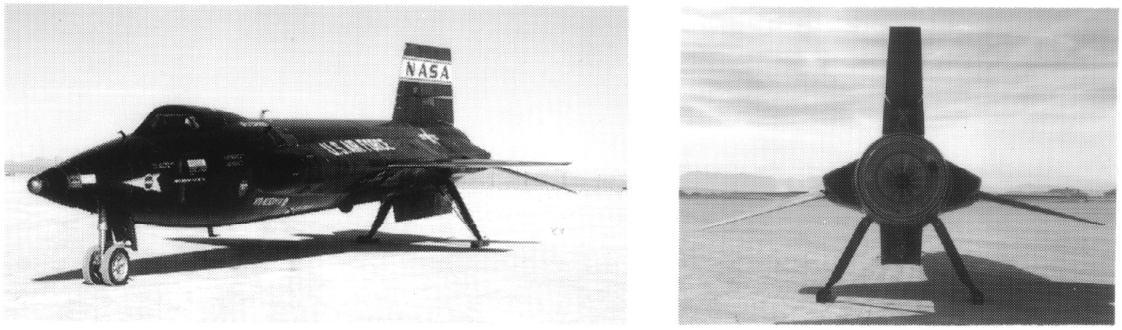

Figure 13. The X-15 research airplane with lower jettisonable ventral fin removed.

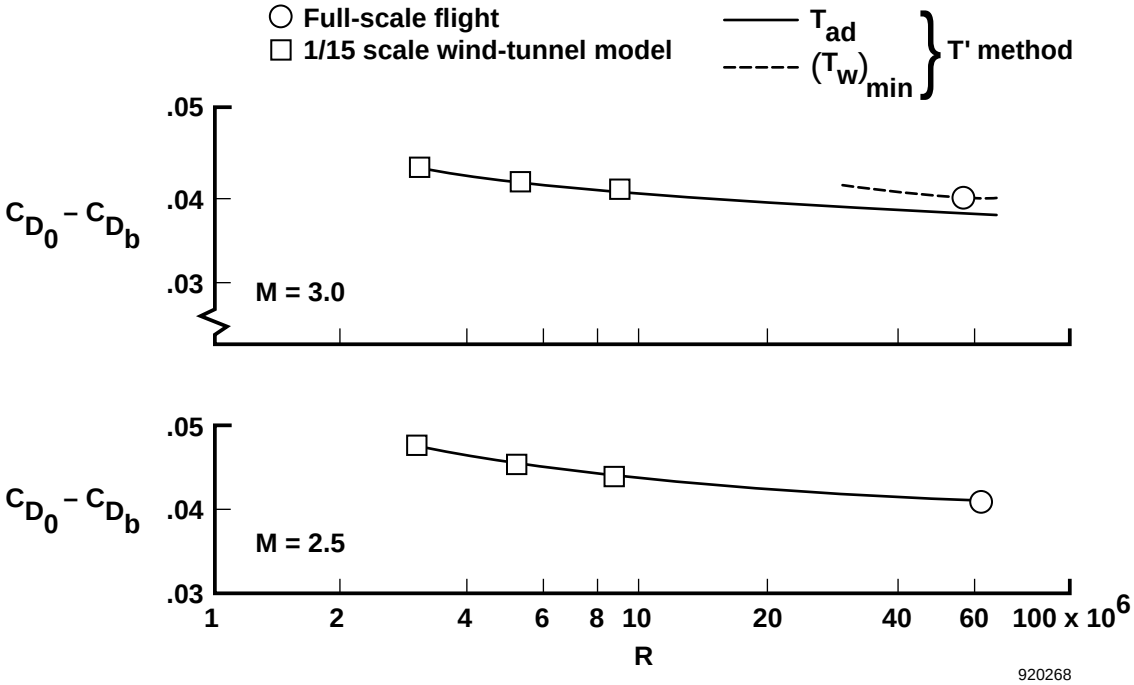

Figure 14. The X-15 flight-to-wind-tunnel model drag correlation.

The base drag had to be subtracted from the zero-lift drag (for each data source) because at these Mach numbers (2.5 and 3.0) the base drag is over 30 percent of the zero-lift drag of the X-15 and model sting support effects biased the base drag of the model. The dashed segment of extrapolated model data for $M = 3.0$ shows the level of drag coefficient that would account for the difference between an adiabatic wall temperature and the minimum wall temperature that was measured for $M = 3.0$ on this flight. Therefore, the level of the flight data (circular symbol) being closer to the dashed segment than to the solid curve is reasonable because it was known that most of the wetted surfaces were below adiabatic temperature. The boundary layer on the model surfaces was tripped at 5 percent of the local chord and 5 percent of the fuselage length.

The good agreement of the extrapolated model data and the full-scale flight data demonstrates the validity of the Sommer and Short *T*-prime extrapolation and confirms the integrity of the wind-tunnel facility, the tunnel test techniques, and the carefully constructed model. This model included all significant external surface details such as antennas, camera fairings, and pitot probes. The overall quality of the model data and the full-scale flight data provided a conclusive correlation of supersonic ground facility and flight determined compressible turbulent-flow viscous drag. This correlation effort also revealed, though the data are not included here, that the model support sting influenced base drag at Mach numbers as high as 3.0.

Wall Interference and Flexibility Effects—The X-15 provided a good correlation of model-to-full-scale flight drag because of configurational simplicity, structural stiffness, the luxury of measuring the drag during power-off (i.e., coasting flight), and careful wind-tunnel testing of a model with reliable

geometry. A much more complex configuration, which was in addition quite flexible, will now be considered with regard to wind-tunnel model-to-full-scale flight lift and drag correlation. Figure 15 shows the subject airplane in flight and lists several physical characteristics.

The large delta-winged XB-70 airplane underwent extensive flight testing during the late 1960's with comprehensive instrumentation for measuring thrust and drag.[32] After the flight tests a rigid 0.03-scale model of the airplane was made to represent the steady-state flexible aircraft shape at M = 2.53. The wind-tunnel model was tested at 14 Mach number–lift combinations corresponding to conditions which were recorded during steady-state flight tests.[33] Another part of this joint effort between NASA centers was provided by a team from the Langley Research Center, who extrapolated the wind-tunnel model results of reference 33 to the previously flown full-scale flight conditions. Predictions were made of control surface deflection effects, inlet spillage, the effects of the boundary-layer trips, Reynolds number effects on skin friction, propulsion system effects, roughness, leakage, interference, and flexibility, and the model base drag was subtracted in favor of flight-measured values. This procedure is reported in reference 34, and the resulting correlation with the flight data is reported in reference 35.

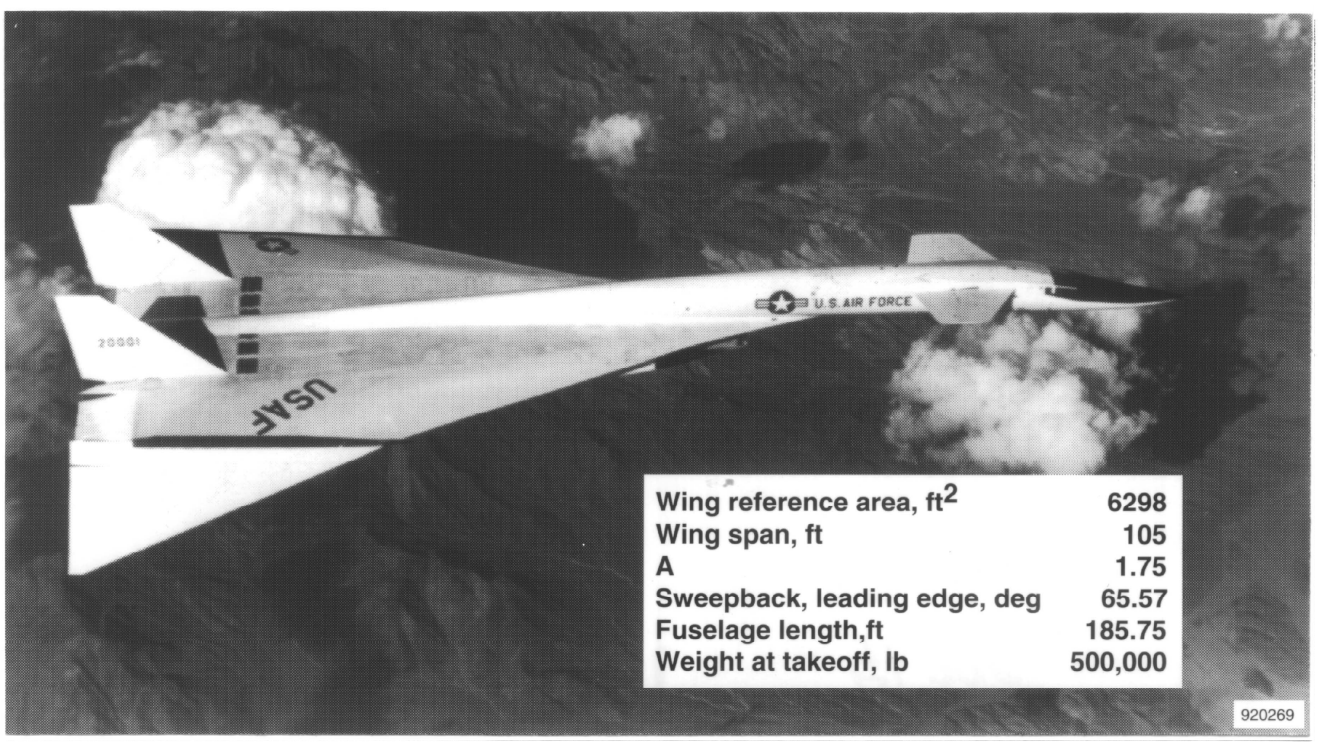

Figure 15. The XB-70 airplane and selected physical characteristics.

Comparisons from reference 35 are shown in figure 16 for the Mach number for which the model was shaped (M = 2.53) and for M = 1.18. The predictions based on model results for the higher Mach number are within 5 percent of the flight drag coefficients for the 1-g conditions ($C_L \approx 0.1$) despite the fact that the prediction of elevon trim was approximately 2° low and that the angle of attack required to generate a specific lift coefficient was under predicted. For M = 1.18 the model-extrapolated drag is

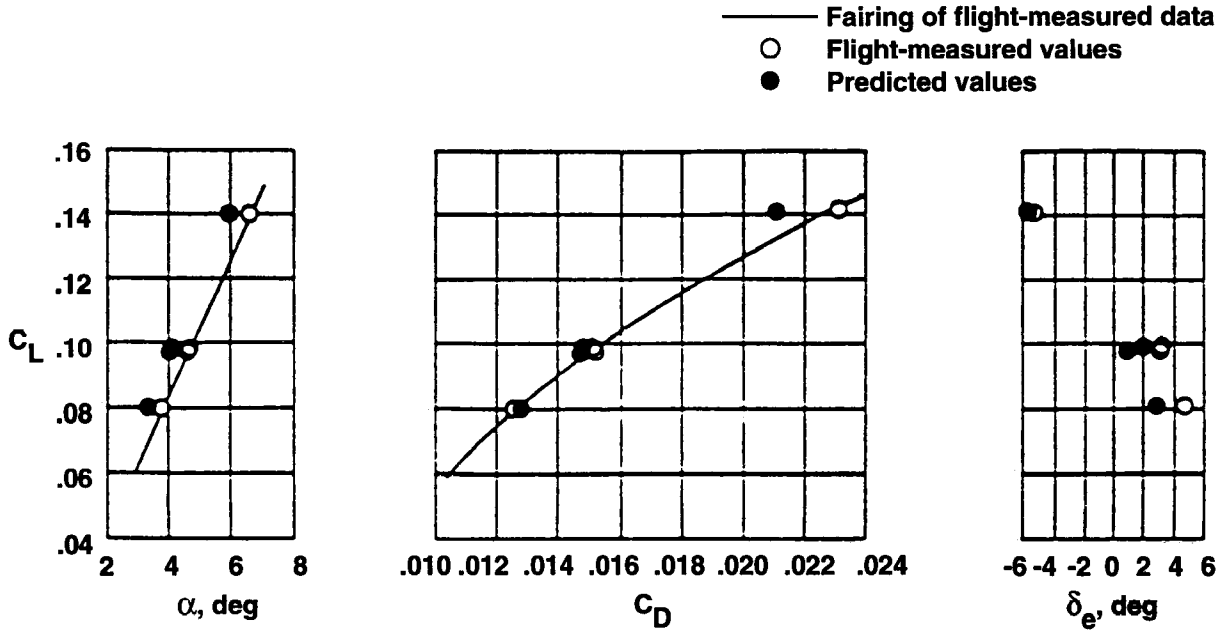

(a) $M = 2.53$

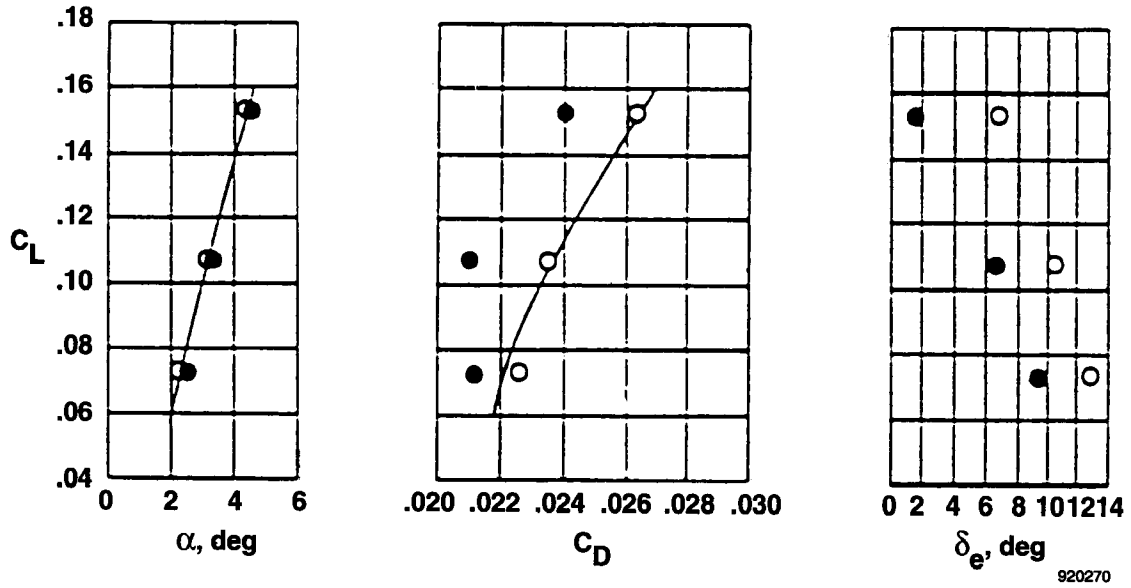

(b) $M = 1.18$.

Figure 16. Lift and drag characteristics of XB-70 airplane at supersonic cruise and transonic conditions, reference 35.

lower than the full-scale flight drag on the order of 10 percent. Corresponding predictions from model data at M = 1.06 (not included here) were approximately 27 percent lower than the flight drag coefficients. These discrepancies for Mach numbers of l.18 and 1.06 may represent wall interference effects on apparent required trim deflections. However, when extrapolated model drag values were adjusted to account for flight-measured trim values, approximately one-third of the drag discrepancy remained for level flight lift conditions. The uncertain effects of flexibility may be a significant part of the remaining drag discrepancy. To achieve this drag correlation it was necessary for the model base drag values in the prediction process to be replaced by the previously measured flight base drag coefficients. The next two paragraphs will explain why this was necessary.

Figure 17 shows an example of how difficult it is to simulate or predict base pressure for an airplane at transonic and low supersonic speeds.[36] The symbols represent a variety of wind-tunnel models having multiple side-by-side jet exhausts which resulted in flattened afterbodies (the XB-70 had six side-by-side turbojet engines and a flattened afterbody). Some models used boattailing and some did not. Models were tested with and without cold air jets for simulating exhaust flow. Comparison of the model data with the eventual full-scale flight results (solid line curve) shows that predictions based on these models would have been prohibitively high in base drag (high negative base pressures produce high base drag).

The designers of the XB-70 were justifiably skeptical of these model results. They were aware that the boundary-layer effects on the models, for the external flow, were poor simulations of full-scale conditions. In addition they had flight experience from a winged missile, having two side-by-side turbojet engines which experienced much lower transonic base drag (the X-10 Navaho missile). The designers pre-flight prediction of the XB-70 base pressure coefficients is represented by the cross-hatch pattern shown in figure 17. The transonic and low supersonic cross-hatch region reflects the X-10 experience and the predicted values at cruise Mach numbers were influenced by the solid square symbols. The solid square symbols were believed to be the model data having the greatest geometric and viscous flow similitude. It is apparent that for most of the supersonic speed range the base drag was poorly predicted, and that the simulation and estimation of base drag for large aircraft, in the region of exhaust jets, is a ask involving great risk. The consequences of faulty estimates are serious for supersonic and hypersonic vehicles.

In summary, the wind-tunnel model data and the flight data, that is, overall drag data, correlate within about 5 percent at the cruise condition where the model was shaped properly. However, uncertainties involving wall interference effects and flexibility were large at transonic and low supersonic speeds where the effects of model shape discrepancies had to be estimated. These uncertainties and higher than expected full-scale base drag contributed to a large transonic drag increment which was a major problem for the XB-70 in that inordinately large amounts of fuel were required to fly through the transonic region when ambient temperature was above standard. The consequences of the transonic wall interference and aircraft flexibility and the difficulty of predicting the transonic base drag, as experienced by the XB-70, should serve as a warning for the promoters and designers of future supersonic and hypersonic aircraft.

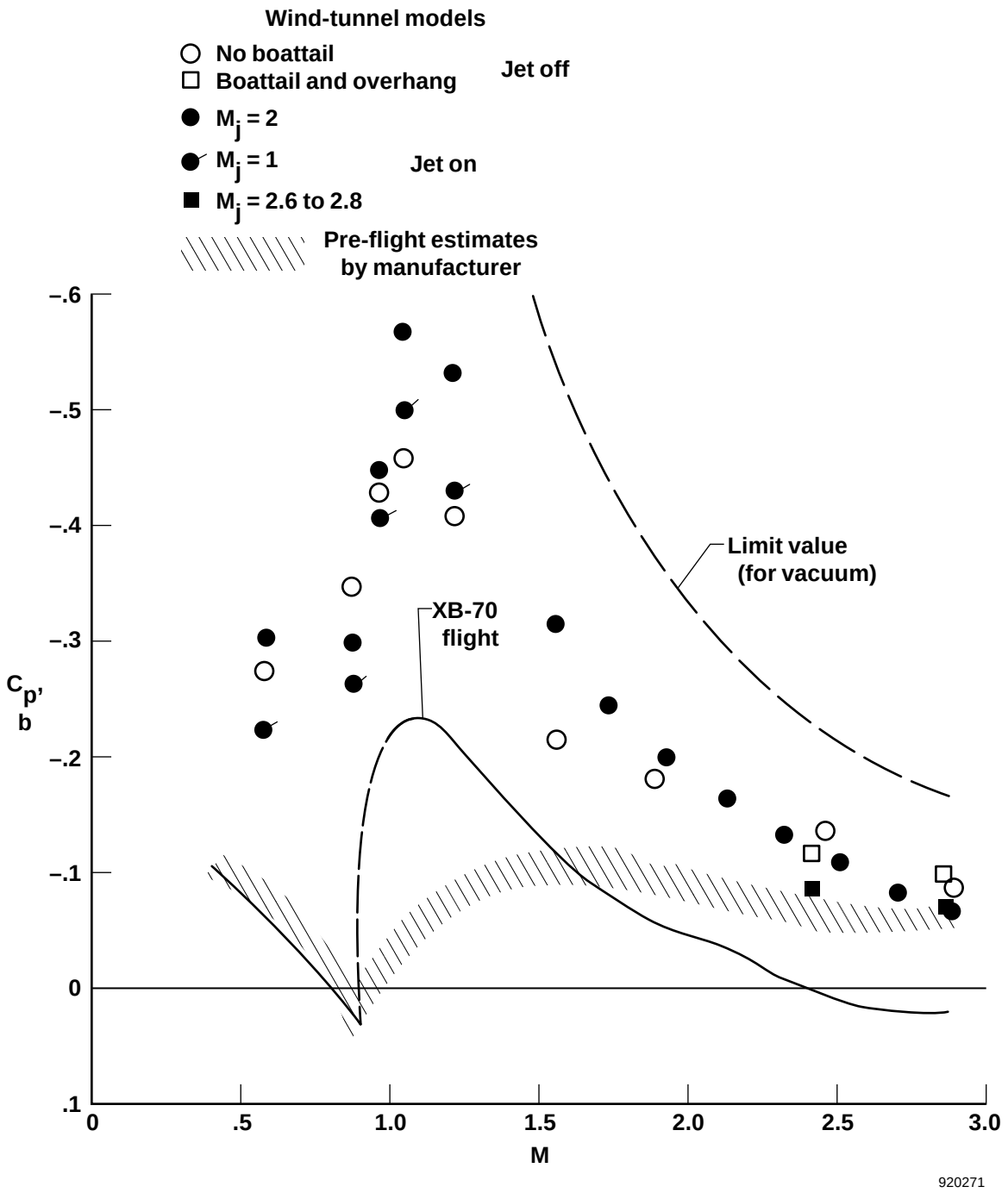

Figure 17. Comparison of flight-measured XB-70 average base pressure coefficient with models having flattened afterbodies, (including cold-air jet flow).

The "Cold-Wall" Experiment: A Direct Wind Tunnel-to-Flight Correlation—During the 1960's attempts were made to obtain in-flight skin friction and heat transfer data at supersonic-to-low hypersonic conditions for correlation with ground facility data and theory. One of the first opportunities for such a correlation was through the use of the X-15 airplane, where high heat transfer rates could be measured on a flat surface at low wall temperatures.[37] More than 10 years after these attempts (and 15 years after the aforementioned X-15 model-to-flight drag correlation), the Dryden facility obtained an airplane which was large enough and fast enough to serve as a test bed for obtaining a more direct wind tunnel-to-flight correlation. The test bed airplane was the YF-12, which could carry the test article to nearly Mach 3.

In a unique cooperative effort between wind-tunnel and flight research teams, a hollow cylinder about 44 cm in diameter and 304 cm long was used to obtain turbulent skin friction data, via a small friction force balance in both environments.[38,39] Notice the hollow cylinder beneath the YF-12 in figure 18. Not only was the same test hardware used in the tunnel and carried in flight, but the same force balance and supporting boundary-layer rake and flush orifice array were used in both environments. The wind-tunnel results for the cylinder[38] were obtained from the NASA Langley Unitary Plan Wind Tunnel.

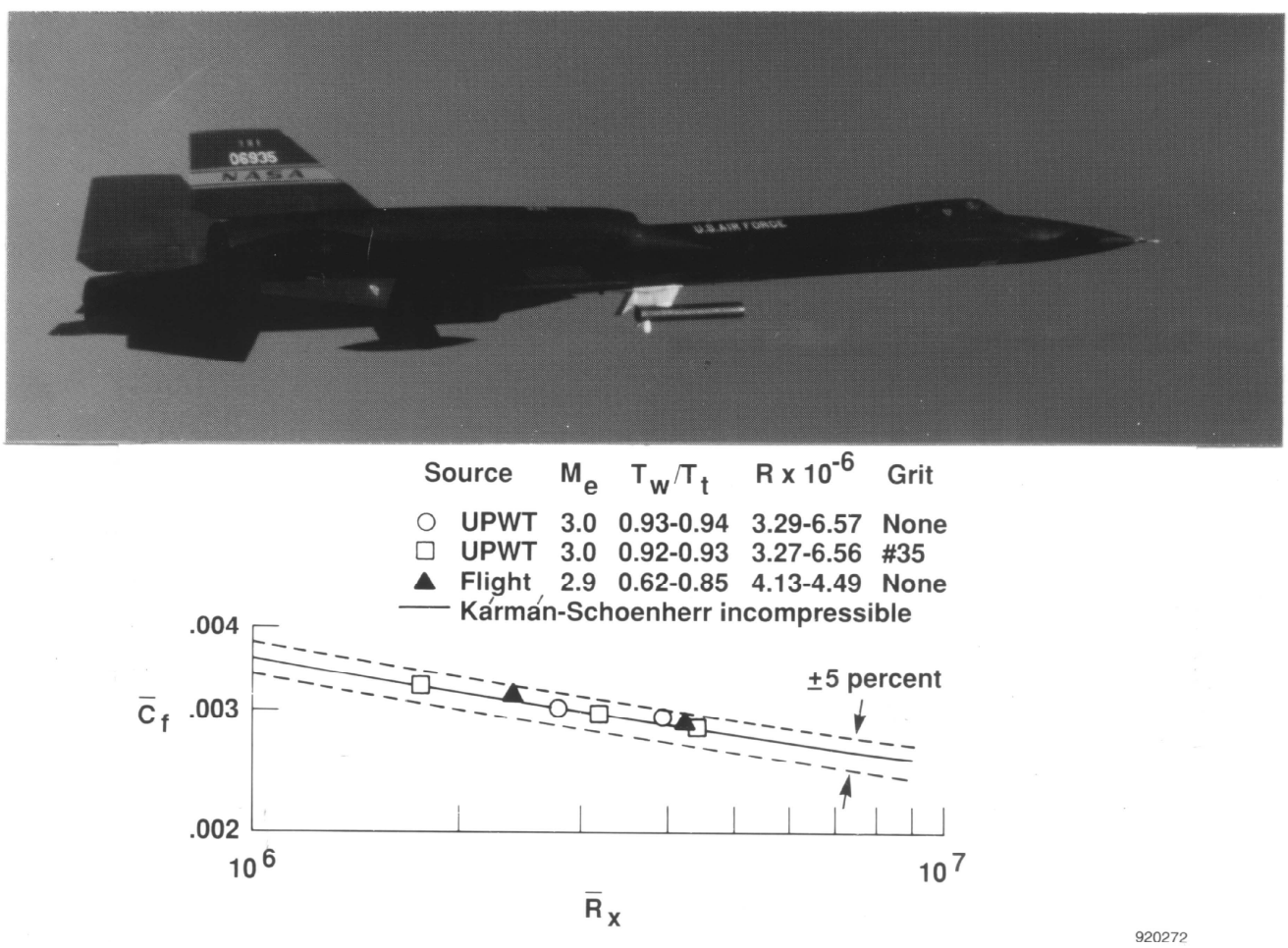

Figure 18. Comparison of local skin friction data obtained from a hollow cylinder in flight and in the wind tunnel, references 38 and 39.

The results, shown in the lower portion of figure 18, indicate that skin friction balance data obtained in flight and from the wind tunnel for M ≈ 3 are in good agreement and both data sources confirm the Kármán-Schoenherr variation of turbulent skin friction with Reynolds number. The transformation of the flight and wind-tunnel data to incompressible conditions for comparison with the incompressible Kármán-Schoenherr curve was achieved through the Sommer and Short *T*-prime reference temperature method previously mentioned.[30,31]

The range of Reynolds numbers obtained in flight was achieved through the differences in wall temperature for the two data points. The flight and tunnel data are very close to the Kármán-Schoenherr curve; the maximum difference being about half, or less, of the ±5-percent increment shown by the dashed curves.

During one flight the cylinder was insulated from the effects of aerodynamic heating while the airplane accelerated to near Mach 3. In addition, the cylinder was cooled with boiloff from a liquid nitrogen source. When the desired steady near-Mach-3 flow conditions were reached the insulation was blown off with primer cord and the extensive instrumentation recorded temperatures, pressures, and a local friction force from which heat transfer and skin friction coefficients could be derived.

Results from the heat transfer measurements were combined with the simultaneous skin friction measurements to obtain an experimental Reynolds analogy factor through the relationship $s = \frac{2St}{C_f}$. Thus the resultant experimental Reynolds analogy factor of 1.11 could be used in the theoretical calculation of heat transfer, avoiding the need to use an estimated value of *s*. A comparison of the measured turbulent heat transfer coefficients and those predicted by the theory of van Driest[40] is shown in figure 19

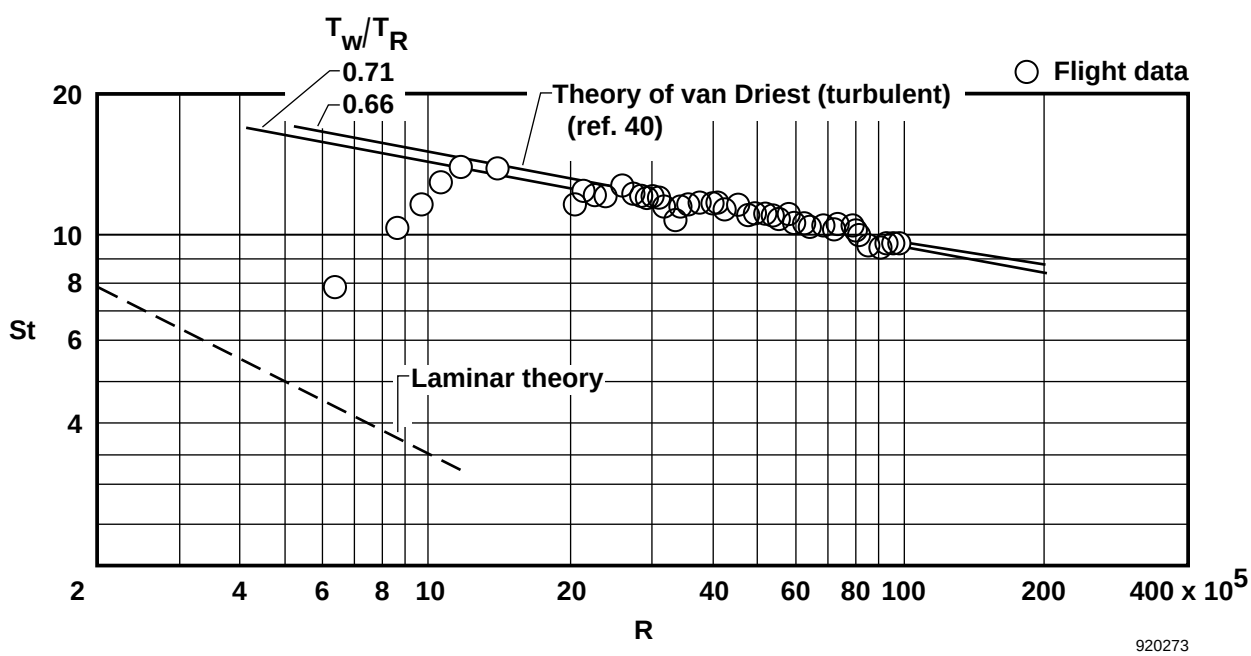

Figure 19. Comparison of measured and calculated heat transfer, local *M* = 2.92, reference 39.

in the form of Stanton number. The two solid lines represent the theoretical Stanton numbers calculated using wall-to-recovery temperature ratios of 0.66 and 0.71 respectively, which correspond to the temperature ratio range that occurred during the heat transfer measurements. The comparison between the flight data and theory shown in figure 19 is considered to be excellent.

This experiment exposed the same test specimen and sensors to the wind-tunnel and flight environments at near-Mach 3 conditions. Recall also, that through the liquid nitrogen cooling scheme, the wall temperature varied rapidly and accurate heat transfer coefficients were thereby obtained. This unique combination of conditions has provided the following important results:

1. An evaluation of five prominent methods for transforming supersonic skin friction coefficients and velocity profiles to incompressible conditions was achieved (see references 38 and 39).

2. Conclusive in-flight confirmation of the magnitude and slope of the Kármán-Schoenherr incompressible relationship of skin friction coefficient and Reynolds number from directly measured friction obtained near Mach 3.

3. A measured Reynolds analogy factor for supersonic speeds in a real flight environment derived from measured skin friction and heat transfer rates.

It is believed that these facts, characterized by the excellent correlations presented in figures 18 and 19, qualify the Cold-Wall Experiment as a benchmark accomplishment in experimental fluid mechanics.

Correlation of Flight and Wind-Tunnel Flow Quality—The experimental determination of the forces and moments, and the distribution of loads from a subscale wind-tunnel model are dependent on a reliable simulation of the full-scale distribution of pressure. This fact was demonstrated early in the history of wind-tunnel experimenting (at low speeds) when it was noticed that different facilities obtained wide ranging values of pressure distribution and drag coefficient for simple airship shapes and spheres.[41] Figure 20, reproduced from reference 41, shows data from prominent experimenters (some pre-World War 1) which prompted the authors, Bacon and Reid, to study and work for an understanding of the erratic nature of the existing data. After careful experimentation in the (then new) Variable Density Wind Tunnel and free-fall tests, the authors concluded, “The tests in free air have demonstrated the fact that no existing wind tunnel can even approximate the nonturbulent condition prevailing in the atmosphere.” That is, they believed that a major source of the discrepancies such as those noted in figure 20 was differing turbulence levels in the air for the respective experiments.

Follow-on experiments[42,43,44] contributed to an understanding of the problem for subsonic tunnels. Dryden and Kuethe[43] developed improved hot-wire anemometer methods that permitted precise definition of turbulence in wind tunnels. After documenting precise flow turbulence levels for the same flow field where they also measured accurate sphere drag values, Dryden and Kuethe established a correlation through the critical Reynolds number (fig. 21). Critical Reynolds number was defined as that value, following the start of boundary-layer transition on the sphere, where the sphere drag coefficient was 0.3. Based on this experience and their conclusive data they postulated that only wind tunnels having the same critical Reynolds number could provide comparable drag results for spheres and airship models.*

*Though the sphere drag tests could now provide a calibration of a wind tunnel for turbulence level, regrettably, all tunnels exceeded the disturbance-free conditions for a body or a sphere traveling through the natural atmosphere.

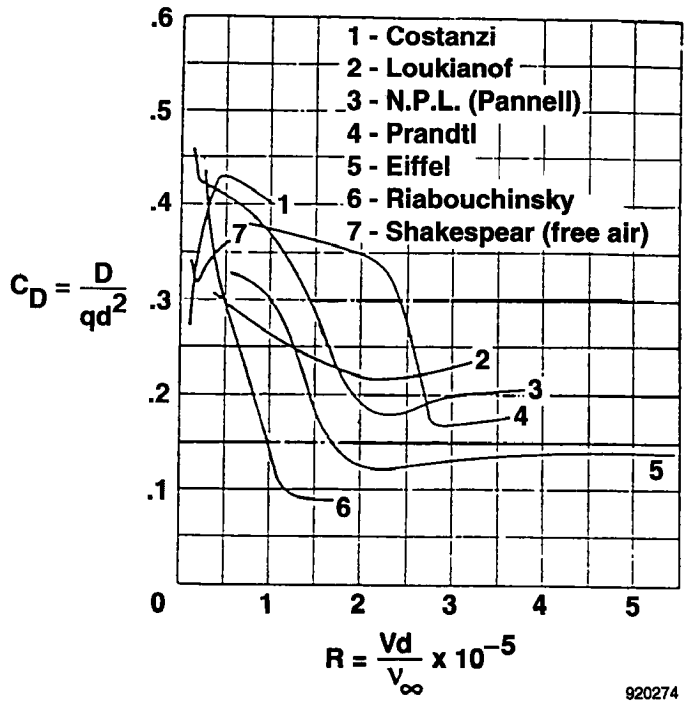

Figure 20. Sphere drag coefficients as a function of Reynolds number, reproduced from reference 41.

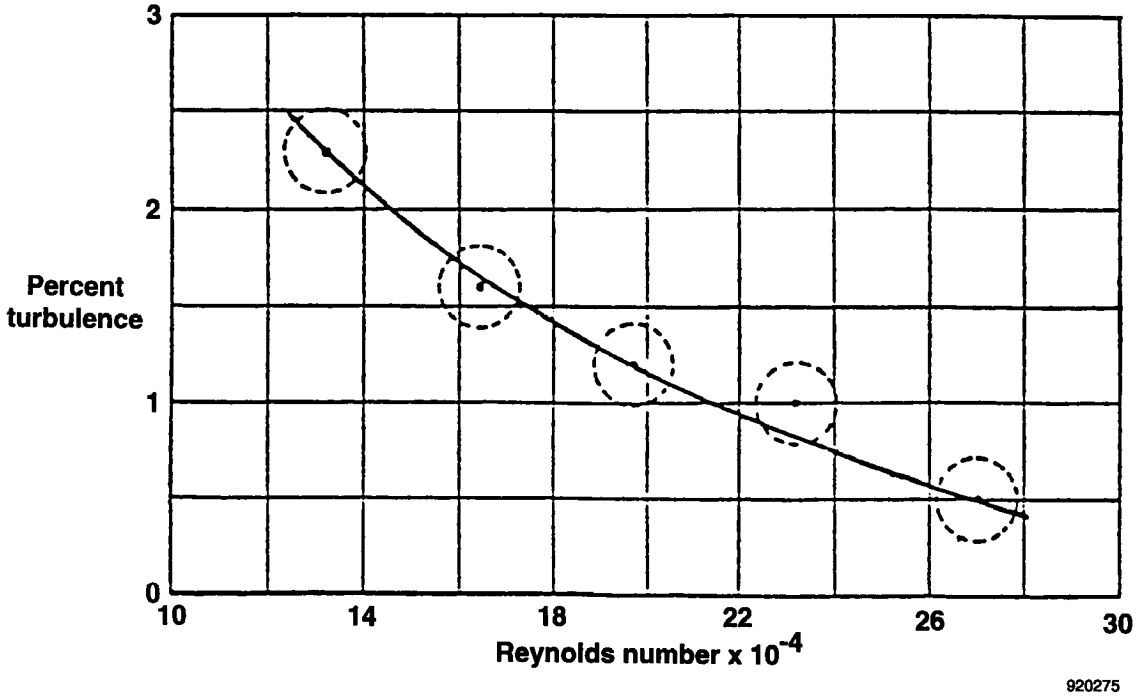

Figure 21. Critical Reynolds numbers of spheres (where C_D = 0.3) as a function of stream turbulence, reference 43.

Thus some order was restored to the art and science of wind-tunnel testing and data interpretation for bodies in subsonic flow. These results were especially useful in defining better shapes for airships, … but, what about model testing at supersonic speeds where shock waves are present? Sphere data would not be applicable for defining the relative turbulence levels at supersonic conditions.

At transonic and supersonic speeds the reliability of the model data depends on whether shock-boundary-layer interactions and areas of flow separation are properly simulated. Such a demanding flow simulation task requires a carefully constructed model immersed in high-quality flow, i.e., freestream flow in the test section having the minimum practical amount of facility-induced noise or turbulence. Unfortunately, the sphere drag methods used at low speeds would not provide comparative turbulence data at supersonic speeds. A new way of defining tunnel turbulence and comparative transition Reynolds numbers was needed.

In the late 1950's, the NACA High-Speed Flight Station became aware of the special quality of the freestream flow in the real flight environment through a unique experiment. A transition Reynolds number of about 8 million had been measured on the lower surface of a specially prepared (fiberglass-covered) F-104 interceptor wing for a Mach number of 2.[45] However, these results only indicated that relatively high transition Reynolds numbers could be obtained in flight at supersonic speeds. They did not provide a solid benchmark as to the relationship of supersonic wind tunnel-to-flight flow quality.

It would be about 20 more years before a unifying experiment would come along which would quantify the relationship of supersonic wind-tunnel and atmospheric flight flow disturbances. This was achieved by testing a precision-made 10°-cone in flight, the same cone that had been used to define the flow quality in 23 wind tunnels (including facilities in three European countries). This supersonic analogy to the subsonic sphere tests was initiated by wind-tunnel experimenters representing the U.S. Air Force Arnold Engineering Development Center (AEDC). After the precision 10°-cone had been used in 23 wind tunnels to define their respective turbulence levels and transition Reynolds numbers, it was installed on a NASA Dryden F-15 airplane. The cone was then exposed to flight conditions over a range of Mach numbers and altitudes. The cone and airplane combination and the cone in a close-up view may be seen in figure 22.

The left portion of figure 23 shows the disturbance parameter (average root-mean-square pressure fluctuation amplitude) as a function of Mach number for the wind tunnels and for the flight environment. The data show that the flow disturbance parameter in the flight environment is significantly lower than the corresponding data from the quieter wind tunnels.[46,47,48]

Transition Reynolds number data from the lower disturbance (quieter) wind tunnels are compared to the flight data in the right-hand portion of figure 23. There was good correlation of transition Reynolds number (specifically end-of-transition Reynolds number) from the quieter wind tunnels and the flight environment up to $M \approx 1.4$. For Mach numbers above 1.4, the correlation deteriorates with the flight environment having significantly higher transition Reynolds numbers. Analogous transition Reynolds number results at some other unit Reynolds numbers show that the flight-to-wind-tunnel correlation deteriorates at slightly lower Mach numbers, near $M = 1.2$.

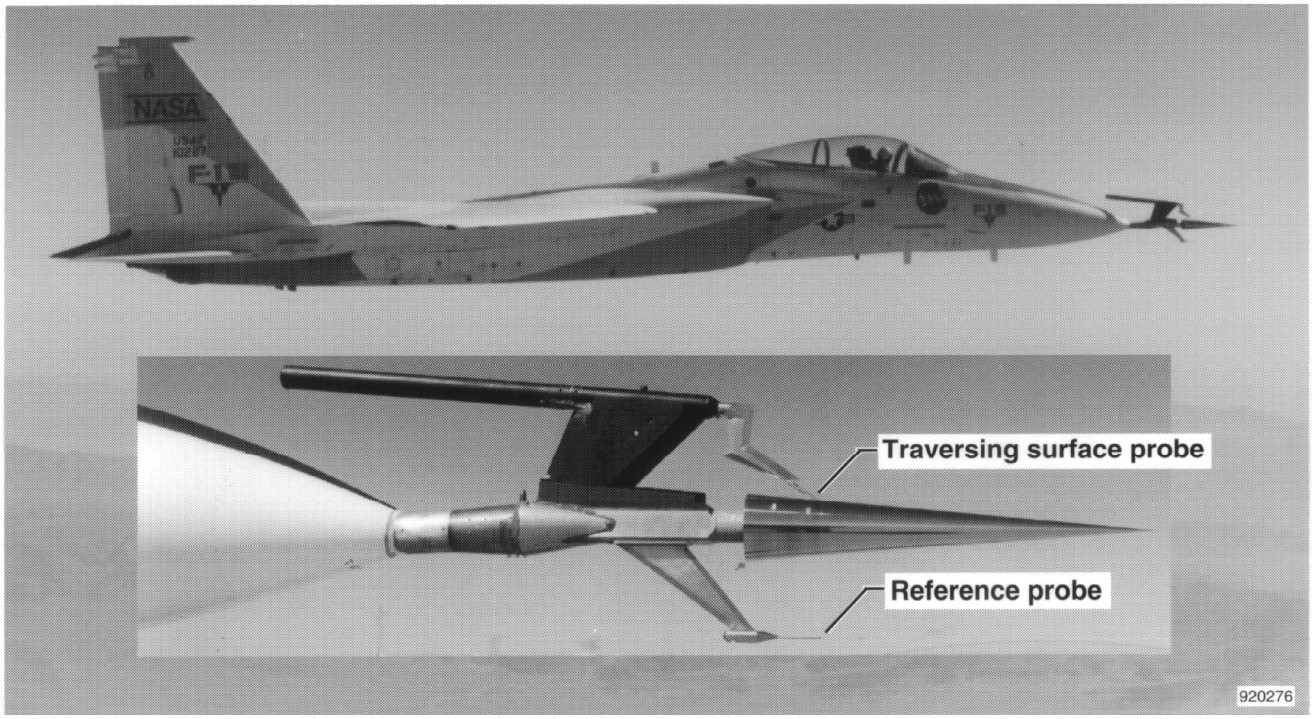

Figure 22. The 10°-research cone as installed on the F-15 airplane.

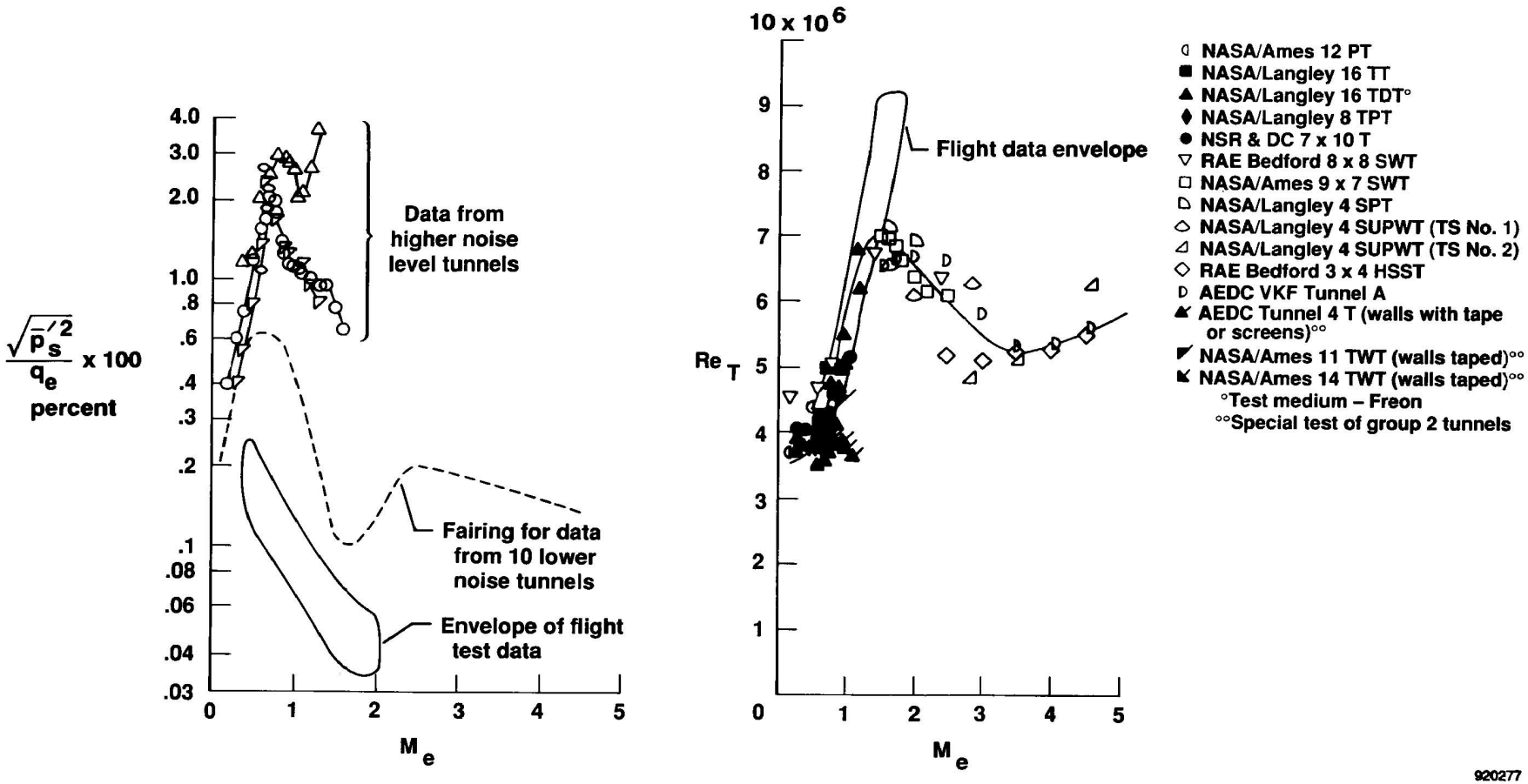

Figure 23. Summary of results from the 10° cone boundary layer transition experiment, zero incidence, adiabatic wall, $U_\infty/\nu_\infty \approx 3.0 \times 10^6$ ft^{-1}.

These results are quite conclusive in that the same test cone, instrumentation, and techniques were used in the wind tunnels and in the flight environment. The many wind-tunnel tests and the flight results comprising this experiment have contributed significantly to a better understanding of the respective test environments and the interpretation of data from same. Stated another way, the flight cone data have provided a benchmark reference for supersonic wind tunnels analogous to the subsonic reference provided by the free-fall sphere tests of the 1920's and 1930's.

Aero-Thermal Structures Research—Thus far the four experiments described in this section have involved aircraft or generic shapes (in the cases of the Cold-Wall cylinder and the 10°-cone) which are evaluated in a flight environment and also tested, or represented by a model, in a wind tunnel. In the present case having to do with structures and the calibration for thermal loads, the flight data are combined with a ground facility of a different sort. The ground facility involved was the Thermostructures Research Facility (TRF), an experimental resource of the aerostructures branch at the NASA DFRF. The following paragraphs describe how the integration of flight data and experimental work in the TRF has provided unique research data toward the definition and isolation of thermal and aerodynamic loads at supersonic speeds.

The measurement of structural loads has been an important part of flight research and flight testing for decades. There have been well established procedures for measuring structural loads by using calibrated strain gauge systems.[49] These methods were applied successfully to aircraft having moderate to relatively high-aspect ratio wings that flew at subsonic or transonic speeds. Such wings were attached to the fuselage at a few discrete locations, consequently, the load paths were well defined and few in number. In addition, at these modest speeds the strain gauge outputs were not compromised by aerodynamic heating.

For aircraft that cruise at supersonic speeds, measuring structural loads is much more complex. The delta planform, for example, results in a significantly longer connection between the wing and fuselage which produces more complex load paths. In addition, at sustained supersonic speeds the strain gauge measurements are contaminated by thermal effects.[50] These effects result from the high temperatures, per se, and also from large thermal gradients which produce thermal stress. To obtain valid loads measurements from an aircraft operating at elevated temperatures, the use of thermally calibrated strain gauges was investigated. This effort used flight tests and laboratory temperature calibrations with the YF-12, a supersonic cruise aircraft having a modified delta planform. Figure 24 shows the structural complexity of the test aircraft. The structural complexity shown therein indicates the difficulty of segregating the aerodynamic and thermal components of flight loads.

The task began by measuring 449 skin temperatures and 112 substructure temperatures during a flight to a Mach number of 3.0. These flight-determined temperature histories were then used to establish the simulation history of temperatures for a laboratory heating test. This consisted of 464 stainless steel panels designed to fit the contours of the aircraft. A schematic representation of how these panels were fitted over (but displaced somewhat away from) the YF-12 surface is given in figure 25. Sixteen thousand, four hundred and thirty (16,430) radiant heater lamps were distributed among the aforementioned panels. A data acquisition system, a control system, and a monitor system together with the previously recorded flight temperature distribution histories permitted the temperature histories to be duplicated in the laboratory under static loading and selected reference loading conditions.[51-56] The lower left part of

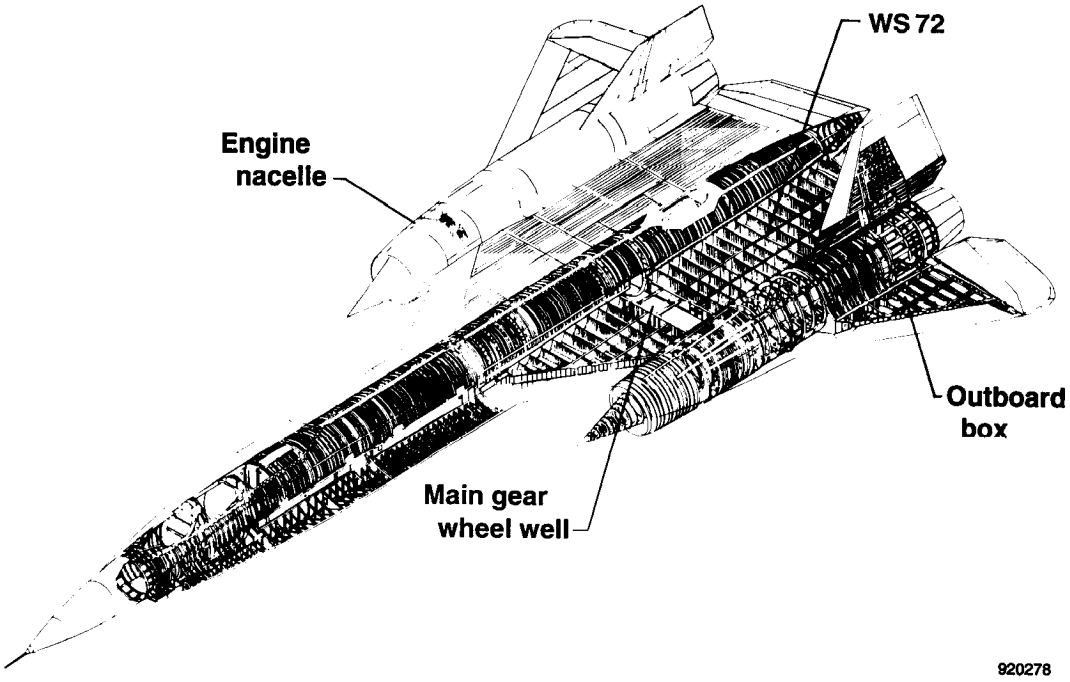

Figure 24. Airplane structure for the YF-12.

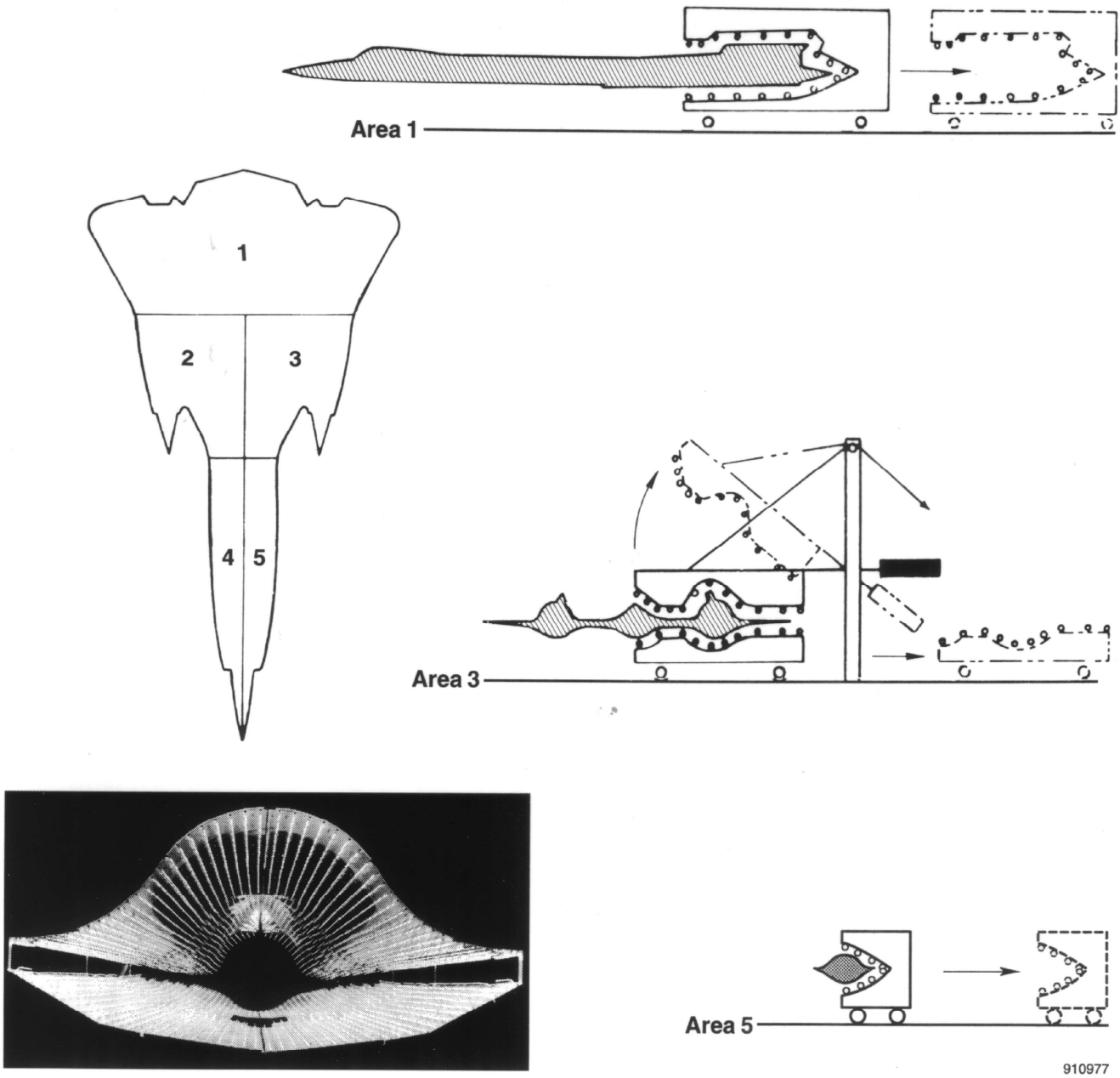

Figure 25. Heater panel configuration for ground based simulation of in-flight heating and photograph of energized heater lamps.

figure 25 shows the illuminated heater lamps, in the absence of the airplane, that would surround the portion of the fuselage forward of the wing.

Figure 26 presents test results which show how strain gauge load equations are affected by thermal stress. This example is representative of the structure joining the outboard wing and nacelle, shown, with the inboard part of the wing. Note the transient behavior of the gauges, which represent the percent of gauge output from thermal effects only, to a 1-*g* cruise reference loading. The foregoing gauge outputs represent the components of torque, shear, and bending moment.

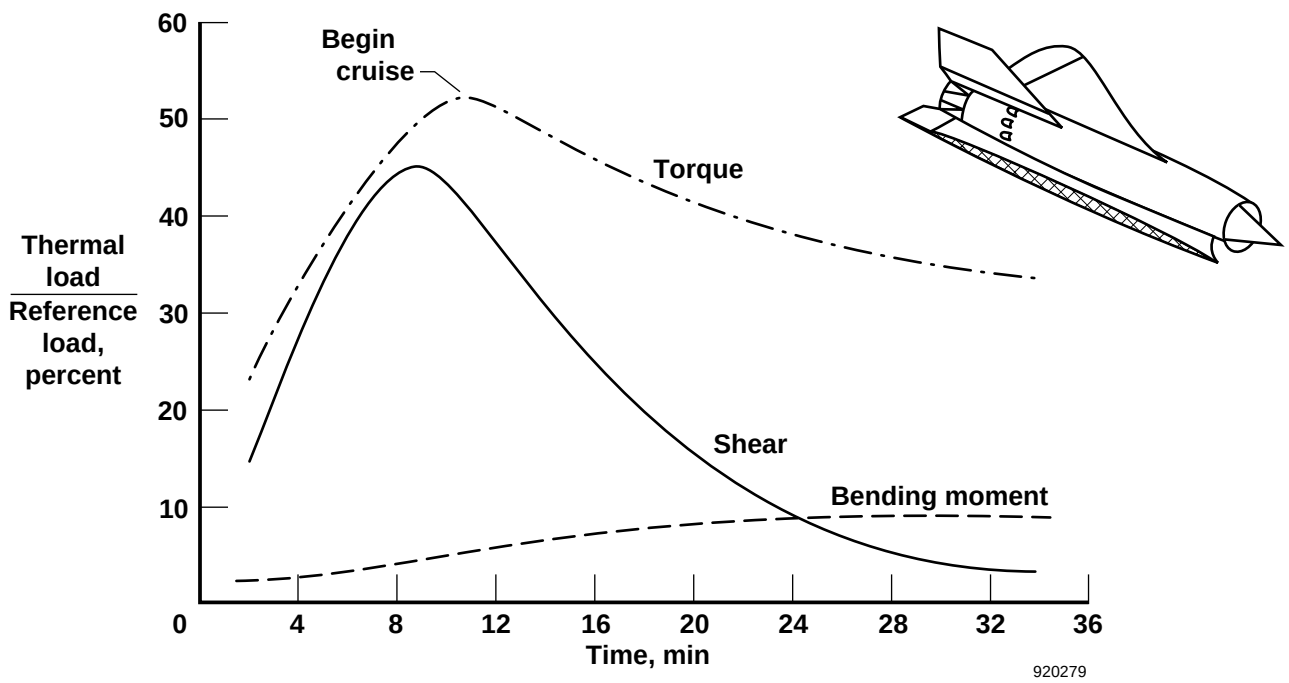

Figure 26. Thermal effects on strain gauge load equations.

Another way of observing the relative thermal component of loading is shown in figure 27 where wing loading is presented in its two components, i.e., the aerodynamic component and the thermal component. Note how the relative magnitude of the two components changes with time.

There were many lessons learned during this rather prodigious structural loads study. Among these lessons we have selected the following to list herein.

- High temperatures <u>and</u> large thermal gradients affect the validity of loads measurements obtained from calibrated strain gauges.
- Nonuniform temperature distributions induce thermal stresses which can be large and which can contaminate flight loads measurements using strain gauges.
- These thermal effects which diminish the validity of strain gauge data at high Mach numbers can be accounted for by thermally calibrating the airplane and the strain gauge system.

This experiment is one of the most complex series of tests ever conducted which combined flight and ground facility techniques and resources. From the resulting unprecedented database, analytical methods were developed for calculating the separation of aerodynamic and thermal loads. The development of this capability is of great importance to the design, structural integrity, and safety of future supersonic and hypersonic aircraft.

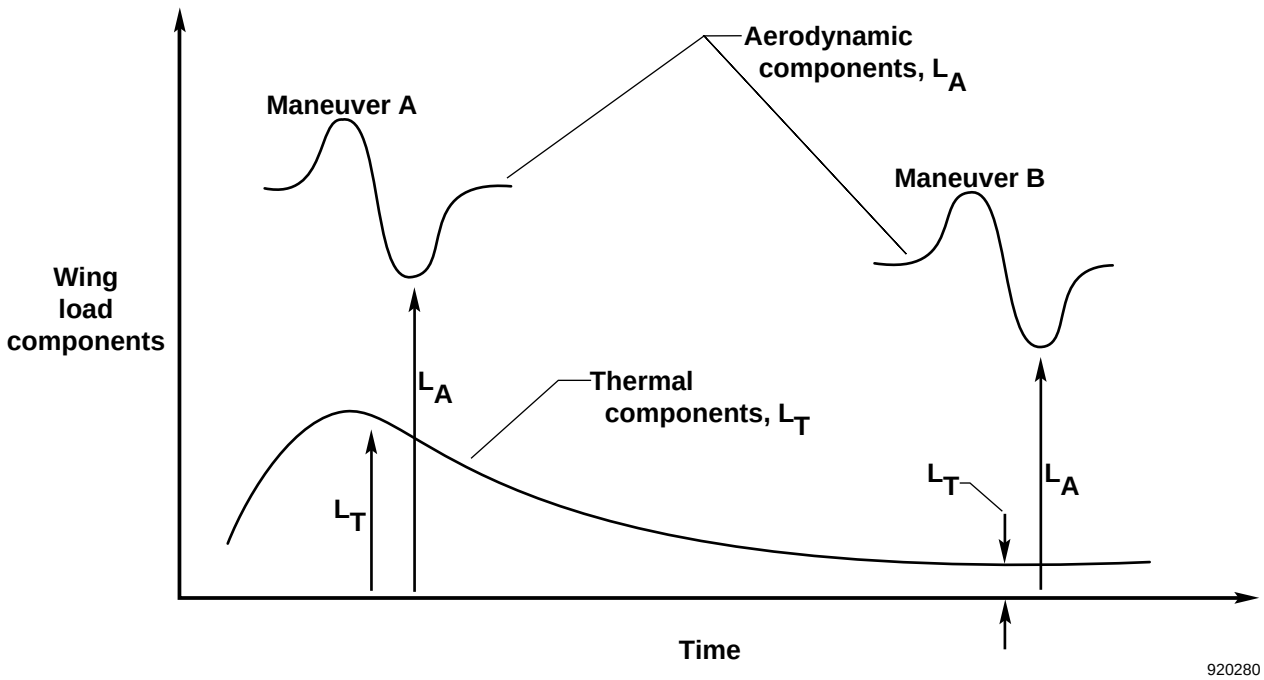

Figure 27. History of aerodynamic and thermal components of load.

Parameter Estimation: A Powerful Tool for Flight-to-Wind-Tunnel Model Data Correlation—The first two experiments described in the "Correlation–Integration" section of this paper pertain to the correlation of axial forces; lift and drag. While these parameters for correlation are important with regard to range and efficiency, analogous correlations for stability and control or handling qualities are more important for aircraft agility and flight safety considerations.

Until the early 1960's stability and control derivatives were extracted using classical techniques such as those included in reference 57. The derivatives were extracted using these (then traditional) techniques for the X-15 research airplane over its entire Mach number range. The resulting flight-derived and wind-tunnel coefficients for the X-15 are given in references 58 and 59. Midway through the X-15 program a more automated technique for obtaining derivatives from flight was developed. Stability derivatives that were previously unobtainable in flight were now extracted by parameter identification, (the maximum likelihood method), references[57,60-62] or parameter estimation techniques. An example from flight tests at NASA–DFRF follows.

Basically the parameter estimation is: given a set of flight time histories of an aircraft response and input variables, find the values of some unknown parameters (coefficients) in the system differential

equations that result in the best representation (fit) of the actual aircraft response. An example of parameter estimation will be shown in the form of histories of several angular rates, displacements, and lateral acceleration for the X-15 airplane at high supersonic Mach numbers.

The left part of figure 28 shows the comparison of the X-15 time histories measured in flight (M = 4.66) and computed by using wind-tunnel predictions. The right part of the same figure shows the X-15 time histories measured in flight and computed by using coefficients obtained from flight data with a maximum likelihood parameter estimation technique (output error method).[57,60] The fit of the two time histories is better for the maximum likelihood technique (especially for r, p, and ϕ), and consequently better values of the coefficients are realized. The coefficients (usually stability and control derivatives) are needed for a variety of uses. Stability and control derivatives estimated from flight data are currently required for correlation studies with predictive techniques (wind tunnel), handling qualities documentation, design compliance, aircraft simulator enhancement and refinement, and control system design and improvement. Correlation, simulation, enhancement and refinement, and control system design applications are discussed in reference 61. Determination of these coefficients has been of major importance for 70 years and a complete discussion of the previously used techniques is given in reference 57. A complete discussion and derivation of the maximum likelihood parameter estimation technique is given in reference 62.

Though the example of parameter estimation given in figure 28 for the X-15 was obtained at the high end of the supersonic speed region, it should be emphasized that the techniques were first attempted, then developed and improved over the entire supersonic range using the X-15 airplane. It was then only natural to use parameter estimation techniques at higher and lower speeds for a variety of aircraft types. The following paragraph discusses parameter estimates (rolling moment due to yaw jets) for the Space Shuttle over a broad range of Mach numbers.

The differences between the predicted and the flight-determined coefficients can be large and knowing the flight-determined values is essential to fixing or understanding undesirable or dangerous flight characteristics. Many examples of understanding flight problems have been documented; 3 are discussed in reference 61. One example taken from reference 61 is shown in figure 29 where the predicted and flight-determined values of the rolling moment due to yaw jets (L_{YJ}) are shown as a function of Mach number. The values of the flight-determined L_{YJ} were included in the update of the simulation resulting in the updated simulation agreeing with the data from future flights.

Other vehicles that have had flight-determined coefficients extracted by maximum likelihood parameter estimation techniques during supersonic flight maneuvers at NASA Dryden are the XB-70, lifting bodies (M2-F3, HL-10, X-24B),[63] F-111A, F-111 transonic aircraft technology (TACT), F-8 digital fly-by-wire (DFBW), F-8 supercritical wing (SCW),[64] YF-12, SR-71, F-14, F-15, F-18, B-1A, highly maneuverable aircraft technology (HiMAT), and X-29. Whereas this listing of aircraft represents those exposed to parameter estimation techniques directly at NASA Dryden, it is known that the safety, flight procedures, and control system design of all current supersonic aircraft have been enhanced by access to parameter estimation techniques.

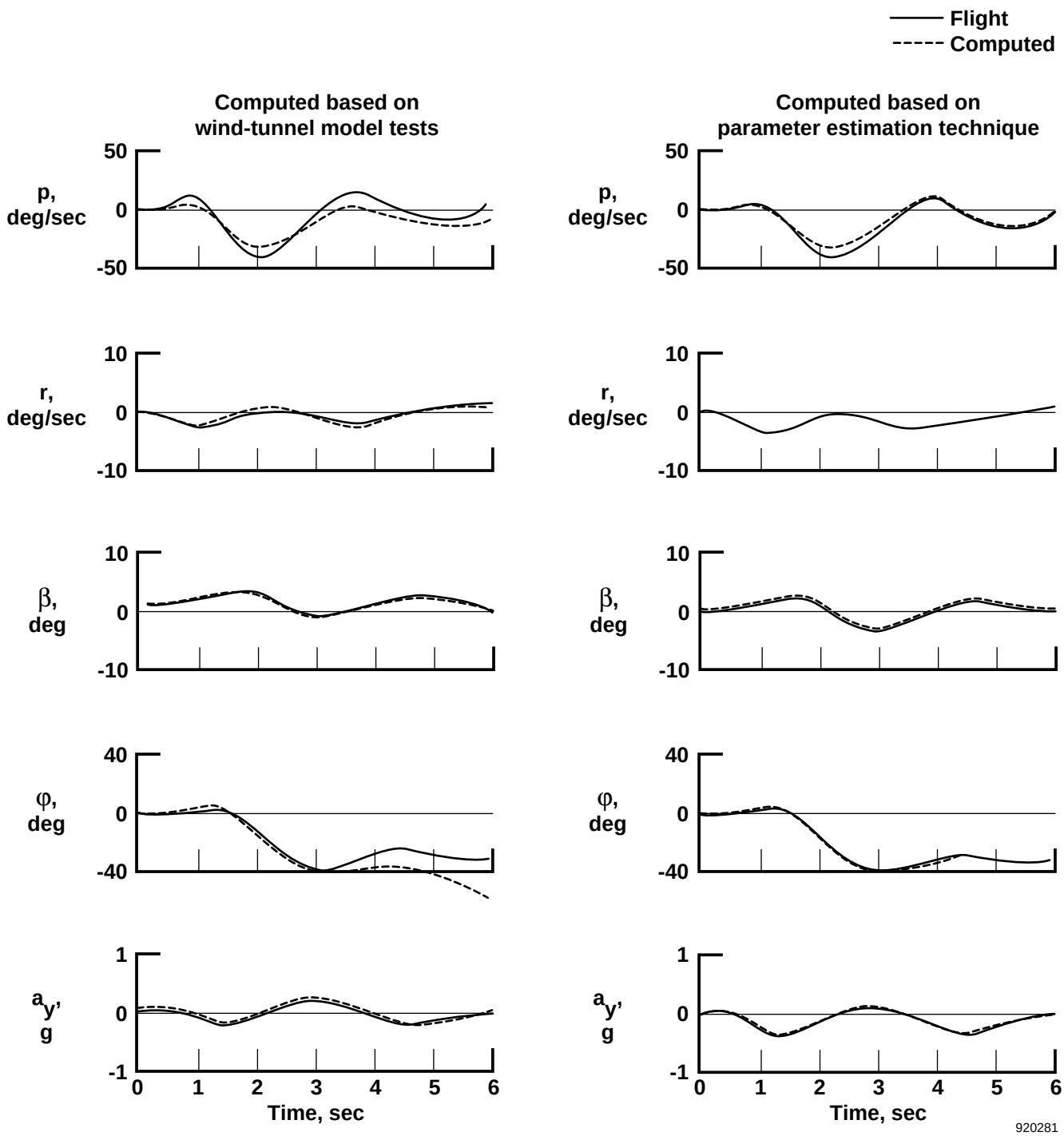

Figure 28. In-flight measured and computed histories for the X-15 airplane, M = 4.66.

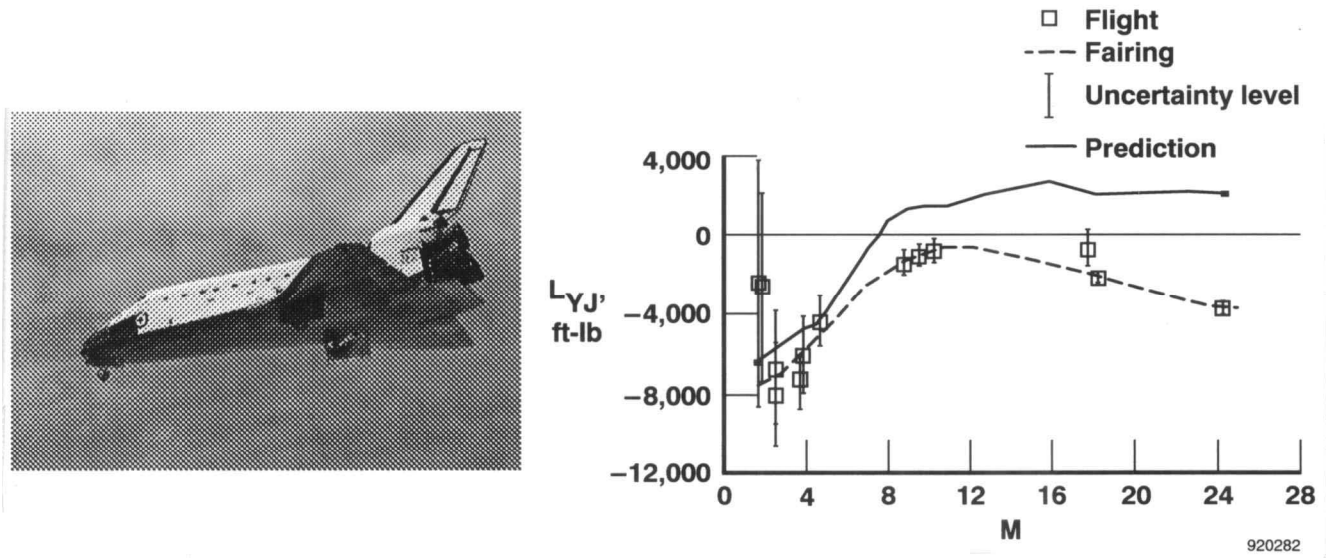

Figure 29. The rolling moment due to yaw jets for the Space Shuttle.

Summary of Stage 2: Correlation–Integration of Ground Facility Data and Flight Data—A common characteristic of these six research items is that each represents a significant improvement in the definition and understanding of the differences between important parameters as derived from flight or from ground facilities. For the first four research items it was found that some ground facility measuring and extrapolation techniques were quite reliable (X-15 drag correlation and cold wall experiment), whereas in other cases serious inadequacies or flow-quality deficiencies were identified in the wind-tunnel results (XB-70 drag correlation and the 10°-cone experiments, respectively).

The aero-thermal structures experiment provided the means to separate the aero loads from the thermal loads in structures for supersonic and hypersonic aircraft. The parameter estimation techniques provide improved safety and flight procedures and will favorably influence control system design for future high-performance aircraft.

Thus, as was also the case for the Stage 1 Barriers to Supersonic Flight experiments, these six research items will also favorably impact the design, performance, efficiency, and safety of future aircraft into the foreseeable future.

It is important to recognize that both aircraft built specifically for research and production aircraft used as test beds or carriers were used to achieve these research results. It is obvious that exclusive reliance on either of the two types of aircraft would have significantly diminished the sum of new supersonic aeronautics knowledge.

Stage 3: Integration of Disciplines

Propulsion Control and Integration—As sustained supersonic flight became more common in the 1960's, the propulsion systems became more complex. Variable geometry inlets and afterburning turbofan engines challenged hydromechanical controls to the limits of their capability.[65] It was expected that future propulsion systems would impose additional requirements on their control systems; such as

- control of more variables,
- increased accuracy and speed,
- integration of control functions, and
- reduced cost.

To accommodate these requirements it was believed that digital control techniques might be a logical approach.

Consequently the U.S. Air Force and NASA initiated a joint program called the integrated propulsion control system (IPCS), using an F-111 airplane.

The F-111 was chosen because it had variable geometry inlets, afterburning turbofan engines, and two engine inlet systems; thus one engine inlet could remain in its normal configuration to ensure flight safety while the other "test" engine inlet system was modified to accept the integrated control concept. In addition to the Air Force and the NASA DFRF, the NASA Lewis Research Center, Boeing (Seattle, WA), and Pratt and Whitney (East Hartford, CT) also had significant roles in this research effort.

New engine control logic as well as engine inlet integration logic was developed. Altitude engine cell tests were conducted at the NASA Lewis facilities followed by flights at Dryden. The flight research obtained through the IPCS digital control system resulted in significant performance improvements.

These included

- faster throttle response,
- stall-free throttle transients, and
- stall-free operation at high Mach numbers.

These benefits and increased performance at supersonic speeds are shown in figure 30, references 65 and 66. In addition to the improved throttle response and stall boundaries the first integrated propulsion control system established the feasibility of

- digital engine control,
- digital inlet control,
- advanced engine control logic, and
- engine inlet integration.

As a result of this pioneering research of integrated propulsion controls there have been follow-on applications and further improvements made to other supersonic aircraft at the Dryden facility. Among the aircraft involved in follow-on applications of integrated propulsion controls is the F-15, which will be discussed in the following paragraphs.

It was on the F-15 airplane that a large step toward digital engine controls was made. This was achieved through the NASA-USAF digital electronic engine control (DEEC) program first flown at

Joint USAF/NASA program

- **Features**
  - **Digital engine control**
  - **Digital inlet control**
  - **Advanced engine control logic**
  - **Engine-inlet integration**

Tests

- **Sea level engine tests**
- **Altitude engine tests at NASA Lewis**
- **27 flights at NASA Dryden**

Payoff

- **Established feasibility of integrated propulsion controls**

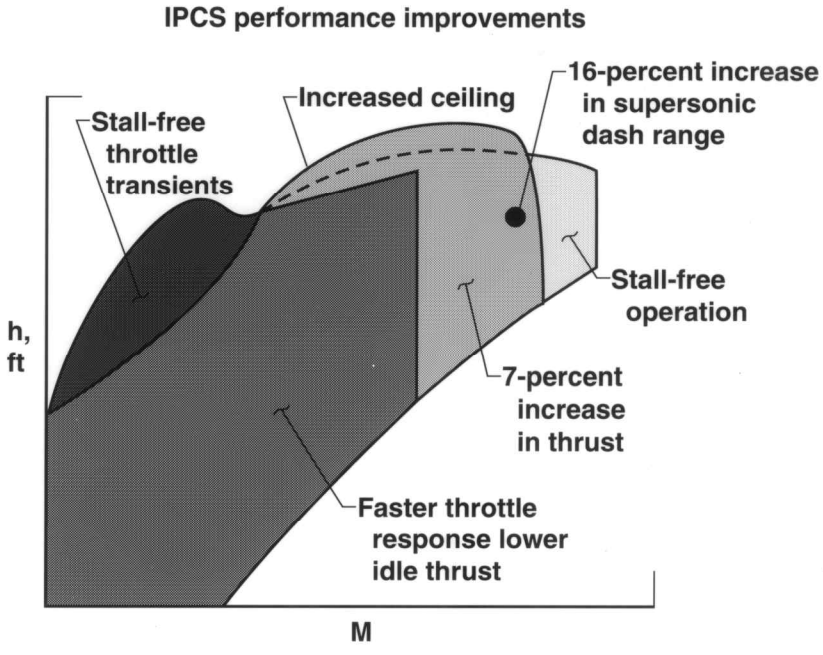

Figure 30. Results from the first in-flight integrated propulsion control system as installed on a modified F-111 airplane.

NASA Dryden.[67] A summary of results from throttle transient tests is shown in figure 31. These results show that the success boundary (that is, the altitude boundary below which compressor stalls did not occur) afforded by DEEC provides increased altitude increments of between 15,000 ft and 10,000 ft depending on Mach number.

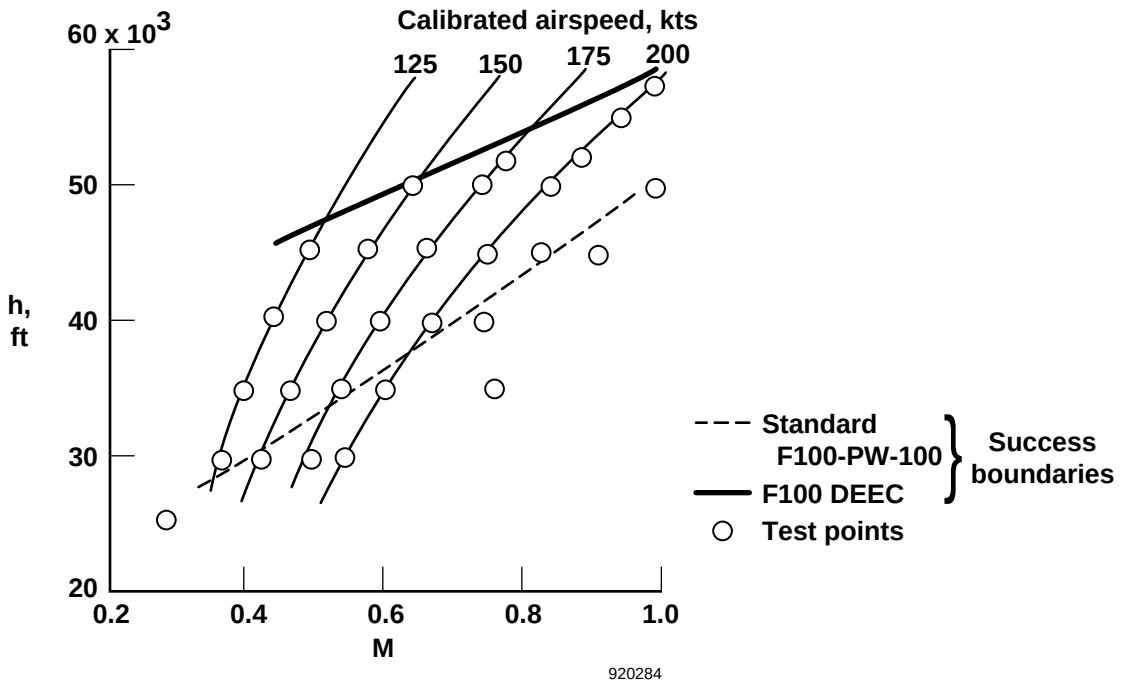

Figure 31. Success boundaries for idle-to-maximum throttle transients for F-15 airplane with and without DEEC modification.

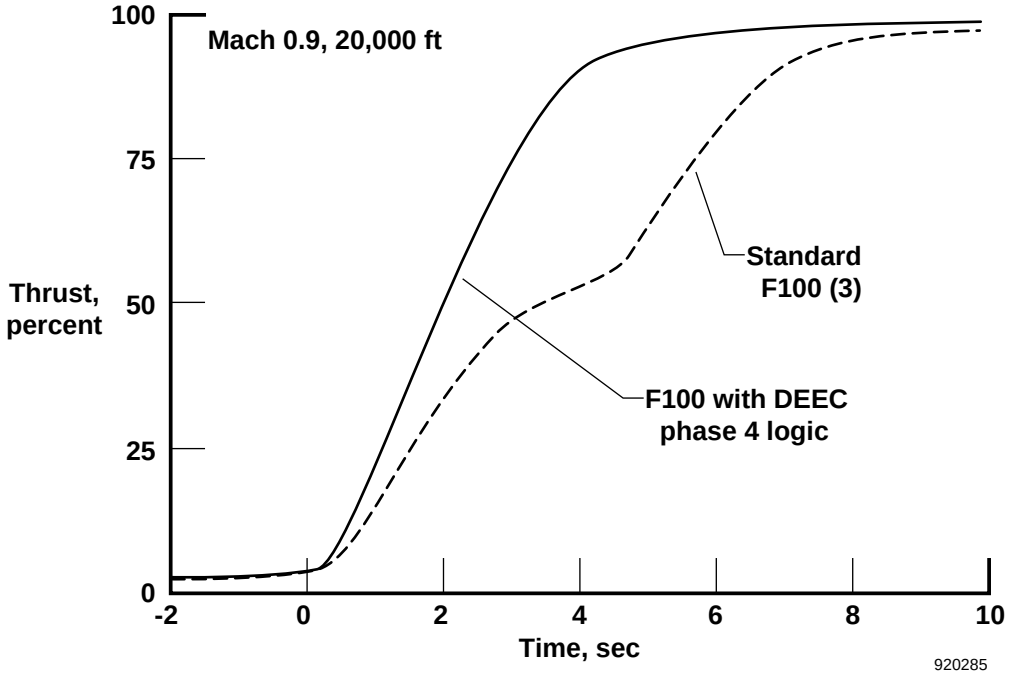

Figure 32. Thrust response for an idle-to-maximum power throttle snap for F-15 airplane with and without DEEC modification.

Figure 32 shows how the DEEC system provided improved thrust response over the standard F100 engine for an idle-to-maximum power throttle snap. The DEEC was highly successful, leading to full-scale development and production of an improved version of the engine, the F100-PW-220. [68] The DEEC also made engine–flight-control integration practical.

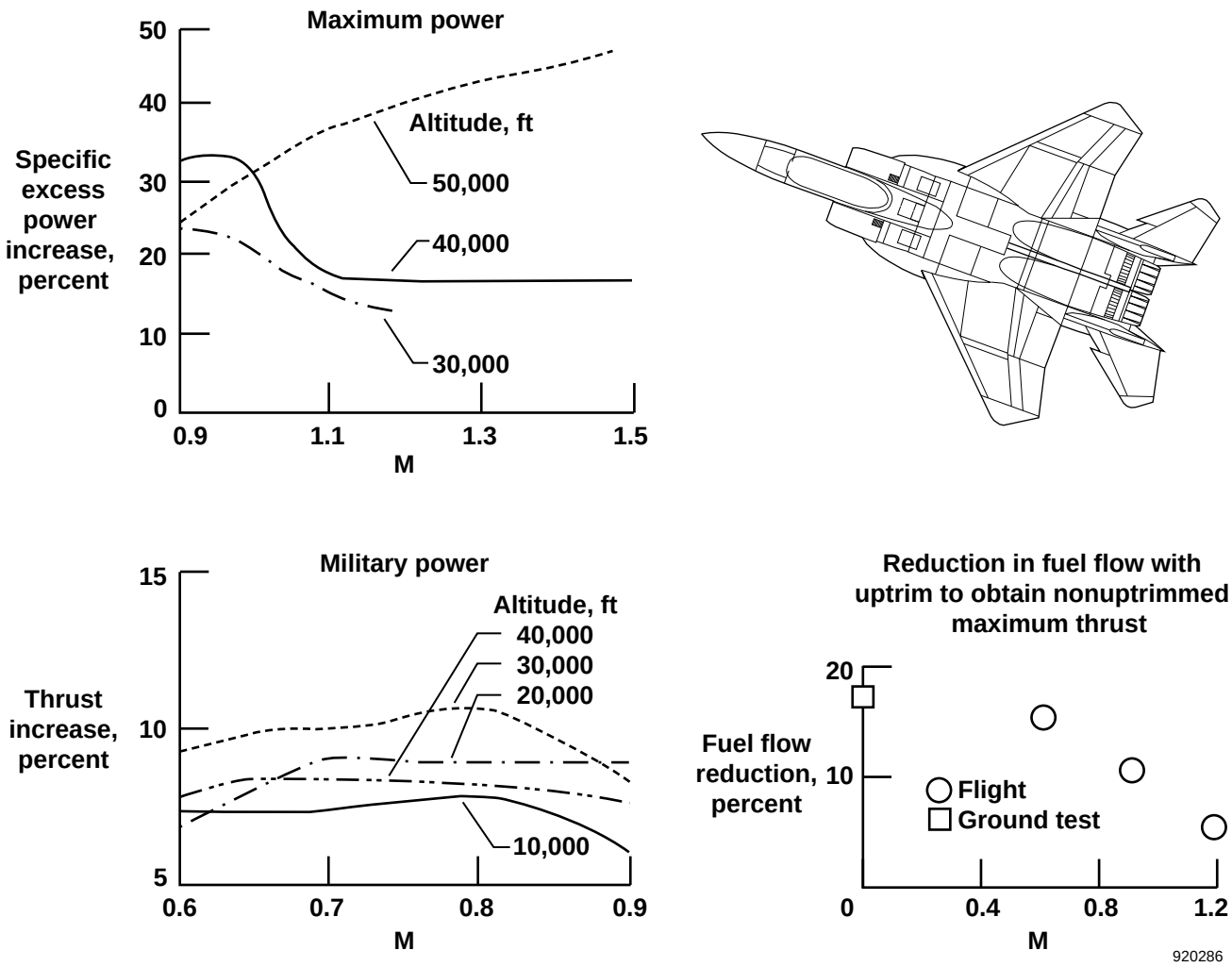

Figure 33. Propulsion–efficiency benefits provided by HIDEC modifications to the F-15 airplane.

The highly integrated digital electronic control (HIDEC) program followed the DEEC experiments.[69] The HIDEC coupled the DEEC to a digital flight-control system which had been added to the F-15 airplane. This allowed the excess engine stall margin to be traded for increased thrust, based on information from the flight-control computer (fig. 33). Also shown in figure 33 are examples of increased specific excess power and reduced fuel flow (5 to 15 percent) for equal thrust. These benefits can be achieved on future aircraft with almost no cost or weight increase.

Thus, the propulsion control integration research begun in the 1970's with IPCS and continued on the F-15 in the 1980's, has clearly achieved its purpose. This technology is ready for use, and as was the case for the technologies described in the Stage 1 section of this report, will favorably impact all future supersonic aircraft.

Mach-Three-Cruise Flightpath Control—For aircraft flying at high altitudes and high speeds (such as advanced supersonic transports or hypersonic cruise vehicles), accurate control of Mach number is necessary for maximum range performance. In the past, subsonic cruise aircraft have usually controlled Mach number through the pitch axis by elevator commands. However, the high altitudes and high speeds associated with supersonic cruise flight contribute to an unfavorable balance between kinetic and potential energy, and when Mach number is controlled through the elevator, large altitude excursions become necessary to correct for small changes in Mach number. The altitude excursions are undesirable from an air traffic control standpoint (current regulations require aircraft to remain within 100 m (300 ft) of a given altitude) and for commercial air passenger comfort as well. Furthermore, such excursions in altitude result in diminished efficiency.

In response to these problems, an altitude and Mach hold control system was developed that operated using elevon and autothrottle control, references 70 and 71 respectively. The system was flight tested at high speeds and altitudes as part of a research program involving YF-12 series aircraft. This improved flightpath control capability was combined with digital control of the inlets and digital airdata and navigation functions in a single digital computer. This permitted operation of the inlet control with smaller margins which improved inlet performance. Range improvements of 7 percent were achieved and inlet unstarts were effectively eliminated.[66,72] One of the airplanes used in this program is shown in figure 34.

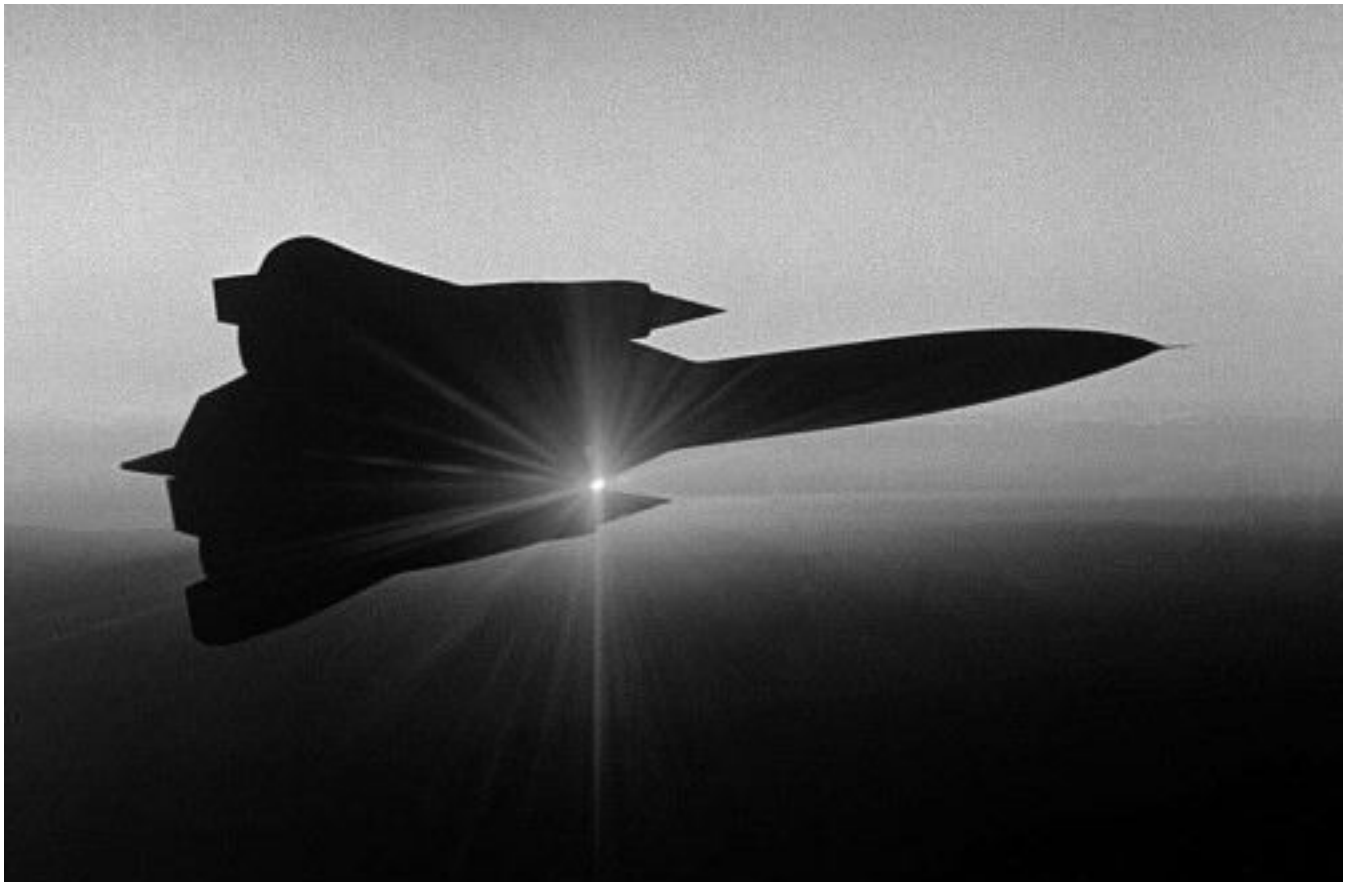

Figure 34. The YF-12C, one of two airplanes used to evaluate the Mach 3 cruise flightpath control concept.

Figure 35 presents flight test data obtained at Mach 3.0 and an altitude of 22,100 m (72,500 ft) with the autothrottle in Mach hold and the pitch autopilot in altitude hold. This particular time history illustrates a number of system response characteristics. The system is in altitude hold at the start of the time history, and the aircraft is stabilized at a bank angle of 36°. Approximately 30 sec into the time history, the autothrottle Mach hold is engaged, and shortly thereafter the aircraft is rolled to wings level. Mach number is well controlled through roll transition and acquisition of stabilized wings-level($\Delta M = \pm 0.01$). Approximately 2.5 min into the run, the pilot commands a 0.023-Mach number reduction (via a potentiometer in the cockpit). Although aircraft response is not rapid, Mach number gradually decreases by the commanded increment. Response is relatively slow, because actuator authority is limited and the error signal has already commanded the minimum power lever angle (PLA). The desired altitude is well maintained before and after rollout, although 24.4 m (80 ft) were gained during the rollout transition. The accuracy of altitude control is particularly noteworthy in view of the large power changes commanded by the autothrottle Mach hold control system. Ride qualities, as indicated by the history of normal acceleration (not shown) are much improved over the conventional Mach hold case. Other relevant literature may be found in references 73 through 76.

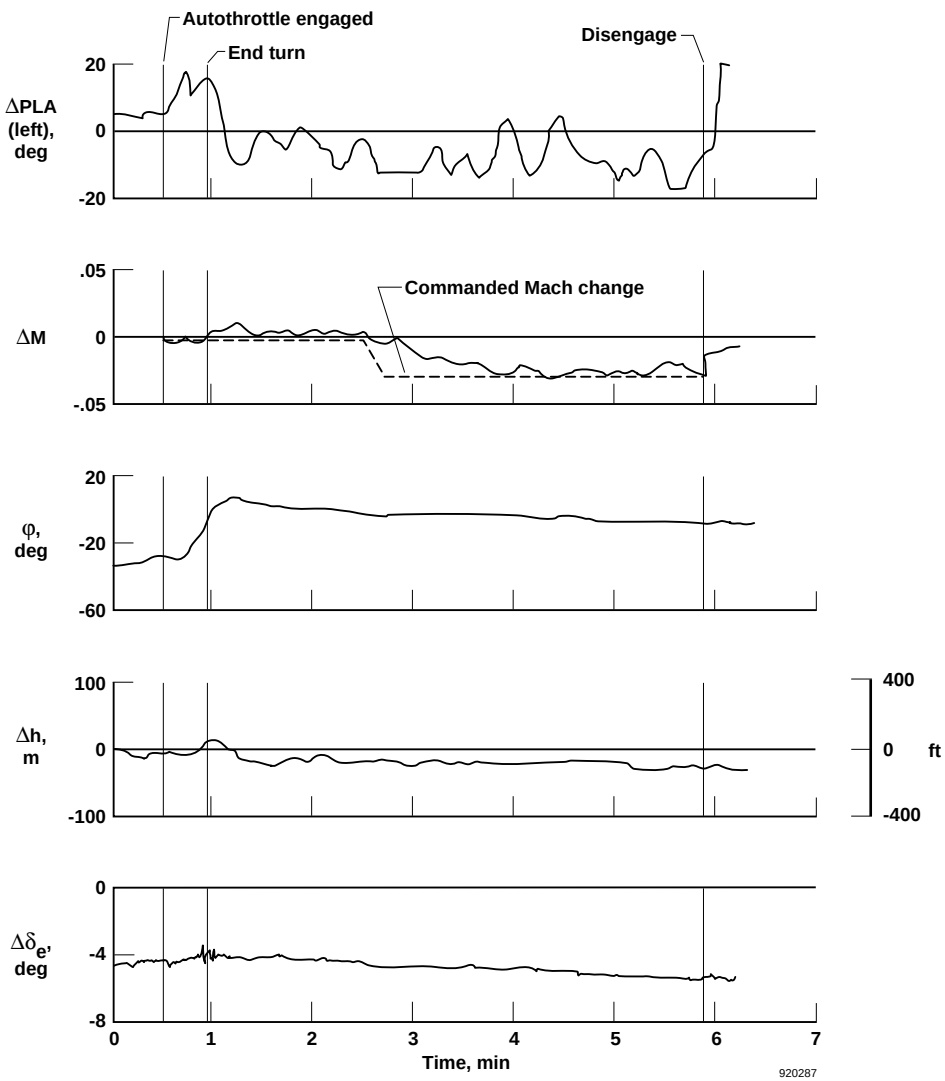

Figure 35. Data history demonstrating autothrottle Mach hold and altitude hold. M = 3.0, h = 72,500 ft.

Digital Fly-By-Wire—The role of electronic flight-control systems has also been a significant factor in achieving increased supersonic performance. Subsonic longitudinal static margin is established based on the required operational range of the center-of-gravity, maneuvering, and stability requirements. The benefits of relaxing longitudinal static margin subsonically, and hence supersonically, even with the aft shift of center-of-pressure, are significant. This was one of the performance advantages foreseen by the (then) Dryden Flight Research Center in the early 1970's, as it embarked on an ambitious program to develop DFBW technology for aircraft. This work culminated in the first DFBW control system for an aircraft in 1972, (without any mechanical backup) using a NASA F-8C research aircraft.[77,78] This airplane, redesignated as the F8-DFBW, is shown in figure 36. In 1976, the first multichannel fault-tolerant DFBW control system was flown in this airplane.[79] This research showed beyond doubt, that traditional aerodynamic stability requirements could be relaxed and traded for performance, using the advanced flight controls to provide the required stability.

This technical milestone provided a new design approach which has been exploited for a number of performance, maneuvering, and mission effectiveness advantages. For the first time, aircraft could be designed with negative longitudinal stability subsonically, which resulted in significantly reduced maneuver drag subsonically, and reduced maneuver and trim drag supersonically.

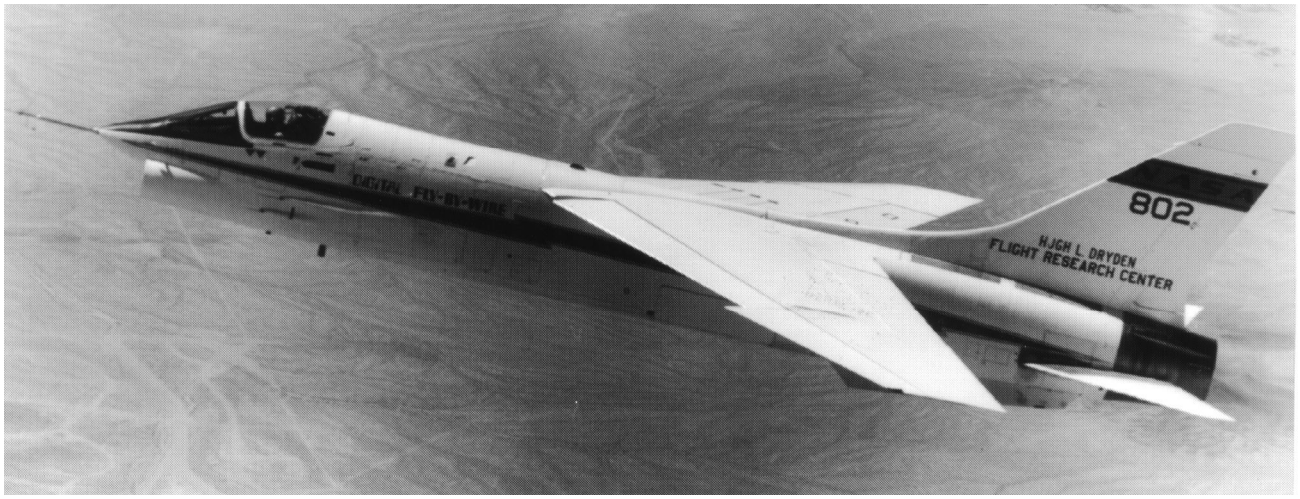

Figure 36. F-8 digital fly-by-wire research airplane.

The full-time, full-authority DFBW control system could provide the static and dynamic stability no longer inherent in the basic aerodynamic design and balance of the aircraft. Such a control system was required by the HiMAT and X-29 research aircraft at their subsonic design points because the time to double amplitude for these aircraft was on the order of 0.25 sec. Without the full-time operation of the electronic control systems, these airplanes would diverge longitudinally (and the X-29, laterally) so quickly that the vehicles would likely be lost in less than 2 sec! Both aircraft demonstrated superior supersonic performance which could not have been achieved had natural longitudinal stability (also lateral for X-29) been required subsonically.

The mechanization of the F8-DFBW control system is shown schematically in figure 37. As explained in reference 79, “A triplex digital computer set containing the control law and system redundancy management software communicates with a specially designed interface unit (IFU).” The IFU processes input data (pilot commands and aircraft sensor signals) and output data (surface commands, cockpit displays, and telemetry data). “The surface commands are routed through a switching mechanism to the servodrive electronics and then to the force-summed secondary actuators.” These are installed in series with the original F-8C actuators. There are five actuator sets; one for each aileron and for each horizontal stabilizer surface and one for the rudder.

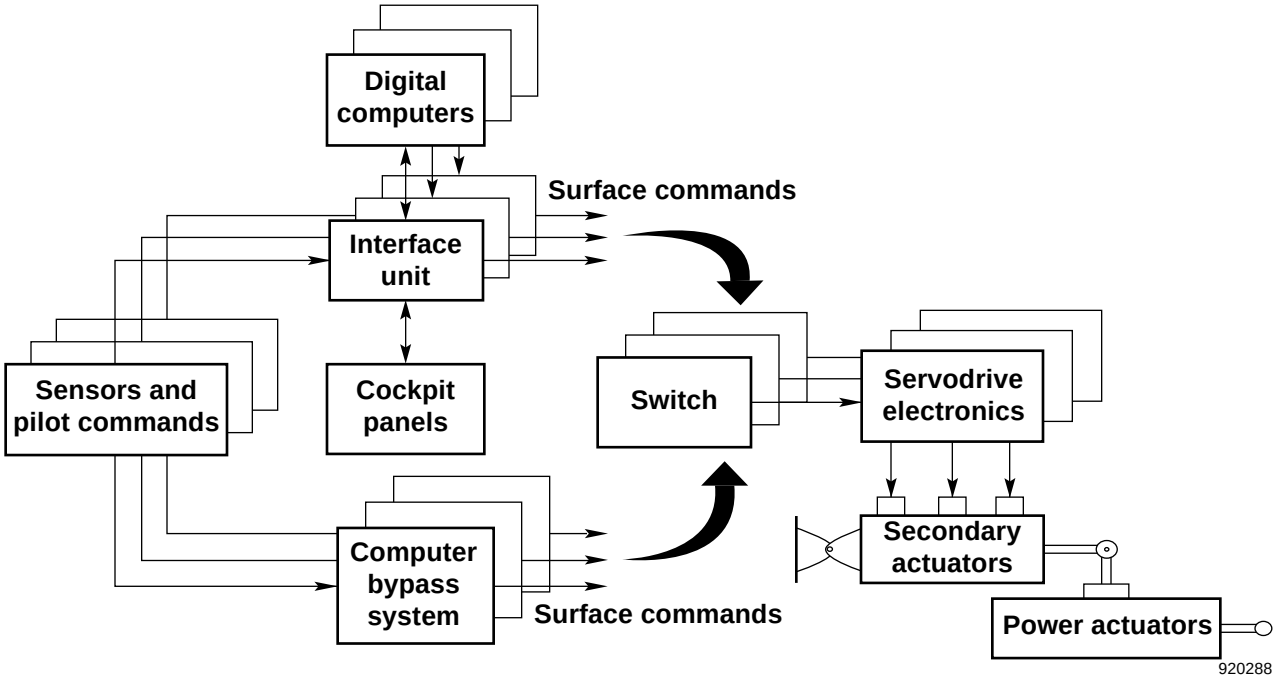

Figure 37. F-8 digital fly-by-wire (DFBW) control system mechanization.

A functional block diagram of the primary digital flight-control system for the F8-DFBW airplane is shown in figure 38. Details regarding this diagram maybe obtained from reference 79. The primary digital flight-control system was backed up by an analog three-axis fly-by-wire control system. The design, development, and flight experience of this backup system are described in reference 80.

The F8-DFBW flight research laid the groundwork, and provided a high level of confidence, for later application of DFBW technology in advanced vehicles such as the Space Shuttle, the F-18, the B-2 Stealth Bomber, the latest models of the F-16, and the next generation of commercial transports.

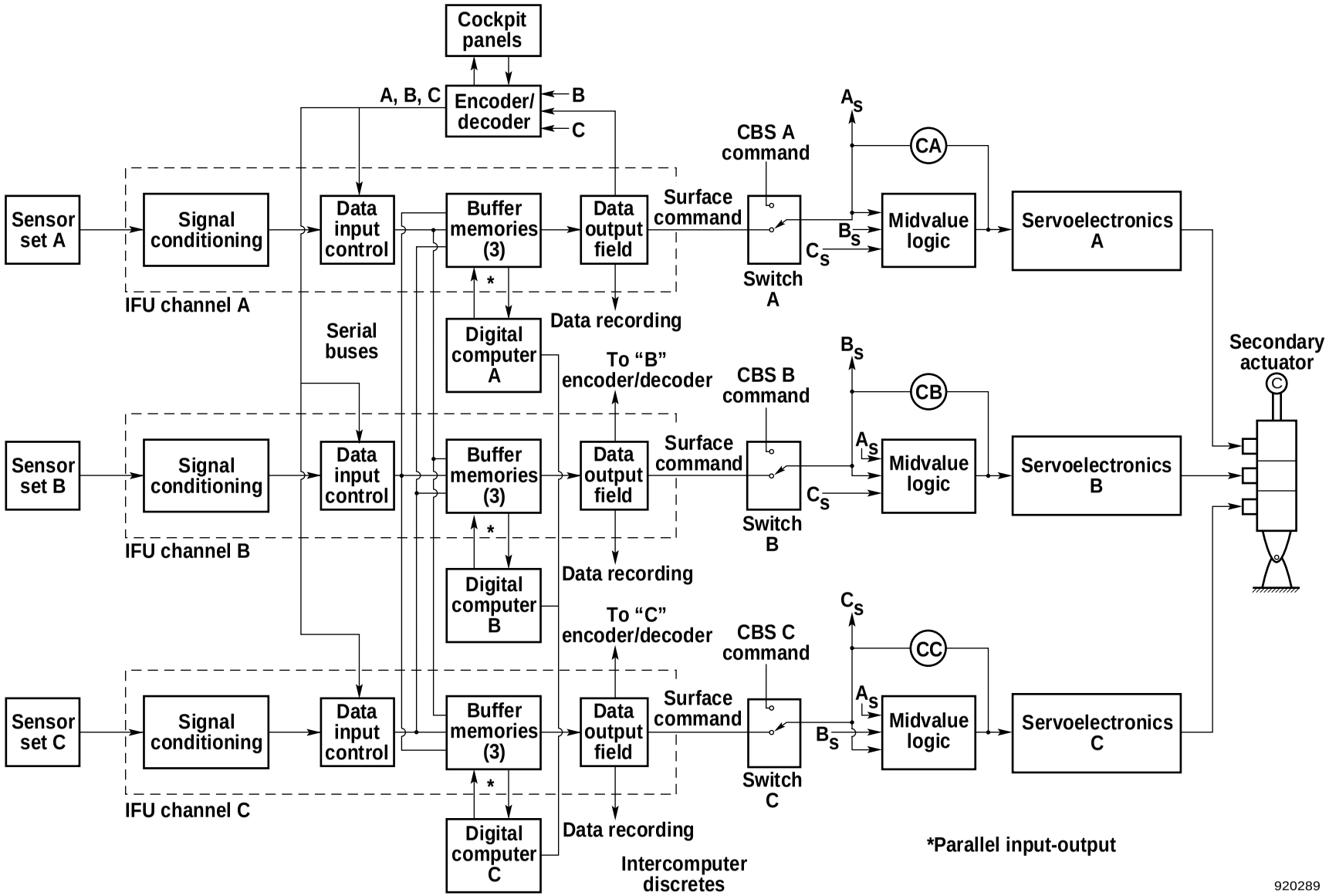

Figure 38. Primary digital system mechanization.

Summary of Stage 3: Integration of Disciplines—As is implied by the heading of this section, these three research items represent a bringing together of various disciplines (aerodynamic, control, electronic, electro-mechanical, hydraulic, and propulsion) in a manner that enhances supersonic flight. The first item (Propulsion Control and Integration) used discipline integration to provide significant improvements of propulsive efficiency. The Mach-Three-Cruise Flightpath Control experiment combined attitude and propulsion control so that ride quality, safety, and efficiency were improved for cruise at "Mach three"; whereas the Digital Fly-By-Wire experiment established static and dynamic stability for a configuration (relative position of center-of-gravity and aerodynamic center) deprived of basic traditional aerodynamic stability. This can favorably influence efficiency and safety of future high-performance aircraft.

Thus it is apparent that each of these three research items yielded results which can provide enhanced safety and efficiency for supersonic aircraft of the future, and that the common thread within these three research items is multidisciplinary integration.

CONCLUDING REMARKS

Thirteen examples of supersonic flight research have been presented which collectively span four decades, beginning in 1946. Approximately one-third of these experiments used unique (experimental or X-series) research aircraft and the remaining experiments used, or were carried by, production type test bed aircraft. The research data and the practical lessons learned from these experiments lead to the following interpretive remarks.

All 13 of the research items presented have demonstrated devices, design principles, techniques, or technology which have had a lasting and favorable influence on aircraft (and some spacecraft) design, safety, reliability, or efficiency. It is reasonable to expect that these favorable influences will continue to be used into the future as long as aircraft and space vehicles are used. Flight research, in concert with theory and ground facility research, has proven to be crucial for assuring safety, reliability, and efficiency of supersonic flight.

The research items described herein have used either unique experimental aircraft (X-series) or production aircraft as test beds. Experience has shown that relying on either type of aircraft exclusively would have significantly diminished our understanding of supersonic flight, supersonic research techniques, and prediction methods.

As would be expected, the nature of supersonic flight research has changed over four decades. Whereas the earlier research items addressed specific barriers or subdisciplines of aeronautics, (Stage 1); the more recent research efforts tend toward the integration of more than one subdiscipline (Stage 3). It is expected, however, that there will be requirements for future flight research that will correspond to each of the three stages discussed herein.

ACKNOWLEDGEMENTS

No technical publication is ever entirely the work of the author, or authors. Even in the case of original research the work, opinions, concepts, or theories of predecessors are used in some capacity. This is especially true for this report. This fact is borne out by the range of aeronautics disciplines considered, the number of references used (80), and the title.

The authors want to acknowledge the technical accomplishments represented by the reference authors whose works provide the technical fabric for this brief summary of supersonic flight research.

In addition, special thanks are expressed to the varied aeronautical specialists of NASA's Dryden Flight Research Facility who supported this publication in numerous ways. This support ranged from the contribution of essential research material (data and sometimes textual), technical review services, advice, and encouragement. The names of these individuals follow in alphabetical order:

Frank W. (Bill) Burcham, Jr., David F. Fisher, Glenn B. Gilyard, Kenneth W. Iliff, Robert Kempel, Wilton P. Lock, Robert D. Quinn, Alexander G. Sim, Kenneth J. Szalai, and Milton O. Thompson.

Reference material, review services, and advice were provided by Richard E. Day, retired from NASA; and a most helpful interview was held with Hubert M. (Jake) Drake, also retired from NASA. In addition, valuable interviews were held with the following flight research–flight test veterans:

C.E. (Bud) Anderson
Donald E. Borchers
Dick Frost
John W. (Jack) Russell

All of these practitioners of aeronautical experimenting (the referenced authors and the individuals explicitly named) have contributed significantly to the substance of this document; and the present authors are indebted to them. The authors are also grateful for the expertise and helpful guidance of their editor, Yvonne D. Kellogg.

Any errors or shortcomings that remain in this document are the responsibility of the authors.

REFERENCES

1. Proceedings of "The European Symposium on Future Supersonic - Hypersonic Transportation Systems," edited by L'Académie Nationale de l'Air et de l'Espace, Strasbourg, France, Nov. 6–8, 1989.

2. Hallion, Richard P., *On The Frontier–Flight Research at Dryden, 1946–1981*, NASA SP-4303, 1984.

3. Hansen, James R., *Engineer In Charge: A History of the Langley Aeronautical Laboratory, 1917–1958*, NASA SP-4305, 1987.

4. “Air Force - NACA Conference on XS-1 Flight Research,” a compilation of the papers presented, Muroc Air Force Base, Muroc, CA, May 19, 1948.

5. Day, Richard E. and Donald Riesert, *Flight Behavior of the X-2 Research Airplane to a Mach Number of 3.20 and a Geometric Altitude of 126,200 Feet*, NASA TM X-137, 1959.

6. Hallion, Richard, *Supersonic Flight, The Story of the Bell X-1 and the Douglas D-558*, Published in association with The Smithsonian Institution, National Air and Space Museum, The Macmillan Company, New York, NY, 1972.

7. Yeager, Charles E., “Operation of the XS-1 Airplane,” 1975 Report of Society of Experimental Test Pilots (SETP) to the Aerospace Profession, pp. 229–235.

8. Williams, Walter C. and Hubert M. Drake, “The Research Airplane - Past, Present and Future,” *Aeronautical Engineering Review*, Jan. 1958, pp. 36–41.

9. *NACA High Speed Flight Station: Flight Experience With Two High-Speed Airplanes Having Violent Lateral–Longitudinal Coupling in Aileron Rolls*, NACA RM H55A13, 1955.

10. Weil, Joseph, Ordway B. Gates, Richard D. Banner, and Albert E. Kuhl, *Flight Experience of Inertia Coupling in Rolling Maneuvers*, NACA RM H55E17b, 1955.

11. Weil, Joseph and Richard E. Day, *An Analog Study of the Relative Importance of Various Factors Affecting Roll Coupling*, NACA RM H56A06, 1956.

12. Weil, Joseph and Richard E. Day, *Correlation of Flight and Analog Investigations of Roll Coupling*, NACA RM H56F08, 1956.

13. Drake, Hubert M. and Wendell H. Stillwell, *Behavior of the Bell X-1A Research Airplane During Exploratory Flights at Mach Numbers Near 2.0 and at Extreme Altitude*s, NACA RM H55G25, 1955.

14. Phillips, William H., *Effect of Steady Rolling on Longitudinal and Directional Stability*, NACA TN 1627, 1948.

15. Drake, Hubert M., Thomas W. Finch, and James R. Peele, *Flight Measurements of Directional Stability to a Mach Number of 1.48 for an Airplane Tested with Three Different Vertical Tail Configurations*, NACA RM H55G26, 1955.

16. Finch, Thomas W., James R. Peele, and Richard E. Day, *Flight Investigation of the Effect of Vertical-Tail Size on the Rolling Behavior of a Swept-Wing Airplane Having Lateral–Longitudinal Coupling*, NACA RM H55L28a, 1956.

17. Becker, John V., *The High-Speed Frontier, Case History of Four NACA Programs, 1920–1950*, NASA SP-445, 1980, pp. 61–118.

18. Wright, Ray H., Virgil S. Ritchie, and Albin O. Pearson, *Characteristics of the Langley 8-Foot Transonic Tunnel with Slotted Test Section*, NACA Report 1389, 1953.

19. Whitcomb, Richard T., *A Study of Zero-Lift Drag-Rise Characteristics of Wing-Body Combinations Near the Speed of Sound*, NACA Report 1273, 1957. (Supersedes NACA RM L52H08, 1952).

20. Donlan, Charles J., *An Assessment of the Airplane Drag Problem at Transonic and Supersonic Speeds*, NACA RM L54F16, 1954.

21. Saltzman, Edwin J. and William P. Asher, *Transonic Flight Evaluation of the Effects of Fuselage Extension and Indentation on the Drag of a 60° Delta-Wing Interceptor Airplane*, NACA RM H57E29, 1957.

22. Whitcomb, Richard T. and Thomas L. Fischetti, *Development of a Supersonic Area Rule and an Application to the Design of a Wing-Body Combination Having High Lift-to-Drag Ratios*, NACA RM L53H31a, 1953.

23. Stillwell, Wendell H., S*tudies of Reaction Controls*, Research-Airplane - Committee Report on Conference on the Progress of the X-15 Project. (a compilation of the papers presented) NACA Langley Aeronautical Laboratory, Langley Field, VA., October 25–26, 1956, pp. 175–181.

24. Holleman, Euclid C. and Wendell H. Stillwell, *Simulator Investigation of Command Reaction Controls*, NACA Conference on High-Speed Aerodynamics, Ames Aeronautical Laboratory, Moffett Field CA, Mar. 18–20, 1958, pp. 157–165.

25. Stillwell, Wendell H. and Hubert M. Drake, *Simulator Studies of Jet Reaction Controls for Use at High Altitude*, NACA RM H58G18a, 1958.

26. Love, James E. and Wendell H. Stillwell, *The Hydrogen-Peroxide Rocket Reaction - Control System for the X-1B Research Airplane*, NASA TN D-185, 1959.

27. Reisert, Donald and Elmor J. Adkins, "Flight and Operational Experiences with Pilot Operated Reaction Controls," *ARS Journal*, Apr. 1962, pp. 626–631.

28. Hopkins, Edward J., David E. Fetterman, Jr., and Edwin J. Saltzman, *Comparison of Full-Scale Lift and Drag Characteristics of the X-15 Airplane With Wind-Tunnel Results and Theory*, NASA TM X-713, 1962.

29. Saltzman, Edwin J. and Darwin J. Garringer, *Summary of Full-Scale Lift and Drag Characteristics of the X-15 Airplane*, NASA TN D-3343, 1966.

30. Sommer, Simon C. and Barbara J. Short, *Free-Flight Measurements of Turbulent-Boundary-Layer Skin Friction in the Presence of Severe Aerodynamic Heating at Mach Numbers From 2.8 to 7.0*, NACA TN 3391, 1955.

31. Peterson, John B., Jr., *A Comparison of Experimental and Theoretical Results for the Compressible Turbulent-Boundary-Layer Skin Friction With Zero Pressure Gradient*, NASA TN D-1795, 1963.

32. Arnaiz, Henry H., *Flight-Measured Lift and Drag Characteristics of a Large, Flexible, High Supersonic Cruise Airplane*, NASA TM X-3532, 1977.

33. Daugherty, James C., *Wind-Tunnel/Flight Correlation Study of Aerodynamic Characteristics of a Large Flexible Supersonic Cruise Airplane (XB-70-1), Vol. I - Wind-Tunnel Tests of a 0.03-Scale Model at Mach Numbers From 0.6 to 2.53*, NASA TP-1514, 1979.

34. Peterson, John B., Jr., Michael J. Mann, Russell B. Sorrells III, Wallace C. Sawyer, and Dennis E. Fuller, *Wind-Tunnel/Flight Correlation Study of Aerodynamic Characteristics of a Large Flexible Supersonic Cruise Airplane (XB-70-1), Vol. II - Extrapolation of Wind-Tunnel Data to Full-Scale Conditions*, NASA TP-1515, 1980.

35. Arnaiz, Henry H., John B. Peterson, Jr., and James C. Daugherty, *Wind-Tunnel/Flight Correlation Study of Aerodynamic Characteristics of a Large Flexible Supersonic Cruise Airplane (XB-70-1). Vol. III - A Comparison Between Characteristics Predicted From Wind-Tunnel Measurements and Those Measured in Flight*, NASA TP-1516, 1980.

36. Saltzman, Edwin J., Sheryll A. Goecke, and Chris Pembo, *Base Pressure Measurements on the XB-70 Airplane at Mach Numbers from 0.4 to 3.0*, NASA TM X-1612, 1968.

37. Quinn, Robert D. and Frank V. Olinger, *Flight-Measured Heat Transfer and Skin Friction at a Mach Number of 5.25 and at Low Wall Temperatures*, NASA TM X-1921, 1969.

38. Stallings, Robert L., Jr. and Milton Lamb, *Wind-Tunnel Measurements and Comparison with Flight of the Boundary Layer and Heat Transfer on a Hollow Cylinder at Mach 3*, NASA TP-1789, 1980.

39. Quinn, Robert D. and Leslie Gong, *In-Flight Boundary-Layer Measurements on a Hollow Cylinder at a Mach Number of 3*.0, NASA TP-1764, 1980.

40. van Driest, E.R., "The Problem of Aerodynamic Heating," *Aeron. Eng. Rev*., Vol. 15, No. 10, Oct. 1956, pp. 26–41.

41. Bacon, David L. and Elliott G. Reid, *The Resistance of Spheres in Wind Tunnels and in Air*, NACA Report 185, 1923.

42. Jacobs, Eastman N., *Sphere Drag Tests in the Variable Density Wind Tunnel*, NACA Technical Note 312, 1929.

43. Dryden, H.L. and A.M. Kuethe, *Effect of Turbulence in Wind Tunnel Measurements*, NACA Report 342, 1930.

44. Platt, Robert C., *Turbulence Factors of N.A.C.A. Wind Tunnels as Determined by Sphere Tests*, NACA Report 558, 1936.

45. Banner, Richard D., John G. McTigue, and Gilbert Petty, Jr., *Boundary-Layer-Transition Measurements in Full-Scale Flight*, NACA RM H58E28, 1958.

46. Fisher, David F. and N. Sam Dougherty, Jr., I*n-Flight Transition Measurement on a 10° Cone at Mach Numbers From 0.5 to 2.0*, NASA TP-1971, 1982.

47. Dougherty, N.S., Jr. and D.F. Fisher, "Boundary Layer Transition on a 10° Cone: Wind Tunnel/Flight Data Correlation," AIAA 80-0154, 18th Aerospace Sciences Meeting, Jan. 14–16, Pasadena, CA, 1980.

48. Fisher, David F. and N. Sam Dougherty, Jr., “Flight and Wind-Tunnel Correlation of Boundary-Layer Transition on the AEDC Transition Cone,” AGARD-CP-339, Flight Mechanics Panel Symposium, Cesme, Turkey, Oct. 11–14, 1982.

49. Skopinski, T.H., William S. Aiken, Jr., and Wilber B. Huston, *Calibration of Strain-Gage Installations in Aircraft Structures for the Measurement of Flight Loads*, NACA Report 1178, 1954.

50. Jenkins, Jerald M. and Albert E. Kuhl, *Recent Load Calibrations Experience with the YF-12 Airplane*, YF-12 Experiments Symposium, Vol. I, NASA CP-2054, 1978, pp. 47–72.

51. Fields, Roger A., *Strain Gage Measurement of Flight Loads at Elevated Temperature*, NASA YF-12 Flight Loads Program, NASA TM X-3061, 1974, pp. 259–302.

52. Sefic, Walter J. and Lawrence F. Reardon, *Loads Calibration of the Airplane*, NASA YF-12 Flight Loads Program, NASA TM X-3061, 1974, pp. 61–107.

53. Jenkins, Jerald M. and Albert E. Kuhl, *Summary of Recent Results Pertaining to Strain Gage Load Measurement Technology on High Speed Aircraft*, NASA YF-12 Flight Loads Program, NASA TM X-3061, 1974, pp. 303–323.

54. Quinn, Robert D. and Frank V. Olinger, *Flight Temperatures and Thermal Simulation Requirements*, NASA YF-12 Flight Loads Program, NASA TM X-3061, 1974, pp. 145–183.

55. Olinger, Frank V., Walter J. Sefic, and Richard J. Rosecrans, *Laboratory Heating Tests of the Airplane*, NASA YF-12 Flight Loads Program, NASA TM X-3061, 1974, pp. 207–257.

56. Jenkins, Jerald M., Albert E. Kuhl, and Alan L. Carter, *The Use of a Simplified Structural Model as an Aid in the Strain Gage Calibration of a Complex Wing*, NASA TM-56046, 1977.

57. Iliff, Kenneth W. and Lawrence W. Taylor, Jr., *Determination of Stability Derivatives from Flight Data Using a Newton-Raphson Minimization Technique*, NASA TN D-6579, 1972.

58. Yancey, Roxanah B., Herman A. Rediess, and Glenn H. Robinson, *Aerodynamic-Derivative Characteristics of the X-15 Research Airplane as Determined from Flight Tests for Mach Numbers From 0.6 To 3.4*, NASA TN D-1060, 1962.

59. Yancey, Roxanah B., *Flight Measurements of Stability and Control Derivatives of the X-15 Research Airplane to a Mach Number of 6.02 and an Angle of Attack of 25°*, NASA TN D-2532, 1964.

60. Taylor, Lawrence W., Jr. and Kenneth W. Iliff, “A Modified Newton-Raphson Method for Determining Stability Derivatives from Flight Data,” 2nd International Conference on Computing Methods in Optimization Problems, San Remo, Italy, Sept. 9–13, 1968, Academic Press, New York, 1969, pp. 353–364.

61. Iliff, Kenneth W., “AIAA Dryden Research Lectureship; Aircraft Parameter Estimation,” AIAA 87-0623, Reno, NV, Jan. 1987.

62. Maine, R.E. and K.W. Iliff, “Identification of Dynamic Systems,” AGARD-AG-300, Vol. 2, 1984. (Also published as NASA RP-1138, 1985.)

63. Sim, Alex G., *A Correlation Between Flight-Determined Derivatives and Wind-Tunnel Data for the X-24B Research Aircraft*, NASA SX-3371, 1976.

64. Iliff, Kenneth W., "Maximum Likelihood Estimation of Lift and Drag from Dynamic Aircraft Maneuvers," *J. Aircraft*, Vol. 14, No. 12, Dec. 1977, pp. 1175–1181.

65. Burcham, Frank W., Jr. and Peter G. Batterton, "Flight Experience with a Digital Integrated Propulsion Control System on an F-111E Airplane," AIAA 76-653, AIAA/SAE 12th Propulsion Conference, Palo Alto, CA, July 26–29, 1976.

66. Burcham, Frank W., Jr., "Propulsion - Flight Control Integration Technology," AGARD-AG-234, Active Controls in Aircraft Design, Nov. 1978, pp. 7–1 to 7–9.

67. Burcham, F.W., Jr., Lawrence P. Myers, and Kevin R. Walsh, "Flight Evaluation of a Digital Electronic Engine Control in an F-15 Airplane," *J. Aircraft*, Vol. 22, No. 12, Dec. 1985, pp. 1072–1078.

68. Burcham, Frank W., Jr., Gary A. Trippensee, David F. Fisher, and Terrill W. Putman, *Summary of Results of NASA F-15 Flight Research Program*, NASA TM-86811, 1986.

69. Myers, Lawrence P. and Kevin R. Walsh, *Performance Improvements of an F-15 Airplane With an Integrated Engine - Flight Control System*, NASA TM-100431, 1988.

70. Gilyard, Glenn B. and John W. Smith, *Results From Flight and Simulator Studies of a Mach 3 Cruise Longitudinal Autopilot*, NASA TP-1180, 1978.

71. Gilyard, Glenn B. and John J. Burken, *Development and Flight Test Results of an Autothrottle Control System at Mach 3 Cruise*, NASA TP-1621, 1980.

72. Reukauf, Paul J. and Frank W. Burcham, Jr., *Propulsion System/Flight Control Integration for Supersonic Aircraft*, NASA CP-001, Supersonic Cruise Aircraft Research (SCAR) Conference, NASA Langley Research Center, Hampton, VA, Nov. 9–12, 1976.

73. Schweikhard, W.G., G.B. Gilyard, J.E. Talbot, and T.W. Brown, "Effects of Atmospheric Conditions on the Operating Characteristics of Supersonic Cruise Aircraft," IAF 76-112, 27th International Astronautical Congress, Anaheim, CA, Oct. 1976.

74. Berry, Donald T. and Bruce G. Powers, "Flying Qualities of a Large, Supersonic Aircraft in Cruise and Landing Approach," AIAA 70-566, May 1970.

75. Berry, D.T. and G.B. Gilyard, "Some Stability and Control Aspects of Airframe/Propulsion System Interactions on the YF-12 Airplane," ASME 73-WA/Aero-4, American Society of Mechanical Engineers, Nov. 1973.

76. Gilyard, Glenn B., Donald T. Berry, and Daumants Belte, *Analysis of a Lateral–Directional Airframe/Propulsion System Interaction*, NASA TM X-2829, 1973.

77. Deets, Dwain A., "Design and Development Experience with a Digital Fly-By-Wire Control System in an F-8 Airplane," Advanced Control Technology and its Potential for Future Transport Aircraft, Los Angeles, CA, July 9–11, 1974. (Also published in NASA TN D-7843, 1975).

78. Szalai, Kenneth J., “Flight Test Experience with the F-8 Digital Fly-By-Wire System; A Forecast for ACT,” Advanced Control Technology and its Potential for Future Transport Aircraft, Los Angeles, CA, July 9–11, 1974. (Also published in NASA TN D-7843, 1975).

79. Szalai, Kenneth J., Phillip G. Felleman, Joseph Gera, and Richard D. Glover, “Design and Test Experience with a Triply Redundant Digital Fly-By-Wire Control System,” AIAA 76-1911, Guidance and Control Conference, San Diego, CA, Aug. 16–18, 1976.

80. Lock, Wilton P., William R. Petersen, and Gaylon B. Whitman, “Mechanization of an Experience with a Triplex Fly-By-Wire Backup Control System,” Advanced Control Technology and its Potential for Future Transport Aircraft, Los Angeles, CA, July 9–11, 1974. (Also published in NASA TN D-7843, 1975).

Listing of stages of supersonic flight research and thirteen selected examples.

Stage 1: Barriers to Supersonic Flight
The Adjustable “All Movable” Stabilizer
The Identification of Inertial Coupling
The Area Rule: Reducing the Magnitude of the Wave Drag Barrier
Reaction Controls: The Problem of Control at Low Dynamic Pressure
Summary of Stage 1
Stage 2: Correlation–Integration of Ground Facility Data and Flight Data
Supersonic Wind-Tunnel Model-to-Flight Drag Correlation
Wall Interference and Flexibility Effects
The “Cold-Wall” Experiment: A Direct Wind-Tunnel-to-Flight Correlation
Correlation of Flight and Wind-Tunnel Flow Quality
Aero-Thermal Structures Research
Parameter Estimation: A Powerful Tool for Flight-to-Wind-Tunnel Model Data Correlation
Summary of Stage 2
Stage 3: Integration of Disciplines
Propulsion Control and Integration
Mach-Three-Cruise Flightpath Control
Digital Fly-By-Wire
Summary of Stage 3

REPORT DOCUMENTATION PAGE

Form Approved
OMB No. 0704-0188

Public reporting burden for this collection of information is estimated to average 1 hour per response, including the time for reviewing instructions, searching existing data sources, gathering and maintaining the data needed, and completing and reviewing the collection of information. Send comments regarding this burden estimate or any other aspect of this collection of information, including suggestions for reducing this burden, to Washington Headquarters Services, Directorate for Information Operations and Reports, 1215 Jefferson Davis Highway, Suite 1204, Arlington, VA 22202-4302, and to the Office of Management and Budget, Paperwork Reduction Project (0704-0188), Washington, DC 20503.

1. AGENCY USE ONLY (Leave blank)

2. REPORT DATE
May 1995

3. REPORT TYPE AND DATES COVERED
NASA SP-513

4. TITLE AND SUBTITLE
Selected Examples of NACA/NASA Supersonic Flight Research

5. FUNDING NUMBERS
010-01-01

6. AUTHOR(S)
Edwin J. Saltzman and Theodore G. Ayers

7. PERFORMING ORGANIZATION NAME(S) AND ADDRESS(ES)
NASA Dryden Flight Research Center
P.O. Box 273
Edwards, California 93523-0273

8. PERFORMING ORGANIZATION REPORT NUMBER
H-1836

9. SPONSORING/MONITORING AGENCY NAME(S) AND ADDRESS(ES)
National Aeronautics and Space Administration
Washington, DC 20546-0001

10. SPONSORING/MONITORING AGENCY REPORT NUMBER
SP-513

11. SUPPLEMENTARY NOTES
Edwin Saltzman: PRC Inc., Edwards, CA 93523-0273;
Theodore Ayers: Dryden Flight Research Center, Edwards, CA 93523-0273

12a. DISTRIBUTION/AVAILABILITY STATEMENT
Unclassified—Unlimited
Subject Category 99

12b. DISTRIBUTION CODE

13. ABSTRACT (Maximum 200 words)

The present Dryden Flight Research Center, a part of the National Aeronautics and Space Administration, has a flight research history that extends back to the mid-1940's. The parent organization was a part of the National Advisory Committee for Aeronautics and was formed in 1946 as the Muroc Flight Test Unit.

This document describes 13 selected examples of important supersonic flight research conducted from the Mojave Desert location of the Dryden Flight Research Center over a 4 decade period beginning in 1946. The research described herein was either obtained at supersonic speeds or enabled subsequent aircraft to penetrate or traverse the supersonic region. In some instances there accrued from these research efforts benefits which are also applicable at lower or higher speed regions. A major consideration in the selection of the various research topics was the lasting impact they have had, or will have, on subsequent supersonic flight vehicle design, efficiency, safety, and performance or upon improved supersonic research techniques.

14. SUBJECT TERMS
Area rule, Compressibility effects, Digital fly-by-wire, Flight path control, Inertial coupling, Model-to-full scale correlation, Parameter estimation, Reaction controls, Supersonic flight research/testing

15. NUMBER OF PAGES
62

16. PRICE CODE
A04

17. SECURITY CLASSIFICATION OF REPORT
Unclassified

18. SECURITY CLASSIFICATION OF THIS PAGE
Unclassified

19. SECURITY CLASSIFICATION OF ABSTRACT
Unclassified

20. LIMITATION OF ABSTRACT
Unlimited

NSN 7540-01-280-5500

Available from the NASA Center for AeroSpace Information, 800 Elkridge Landing Road, Linthicum Heights, MD 21090; (301)621-0390

Standard Form 298 (Rev. 2-89)
Prescribed by ANSI Std. Z39-18
298-102